Full-Duplex Communication for ISAC: Joint Beamforming and Power Optimization

Zhenyao He, Wei Xu, *Senior Member, IEEE,* Hong Shen, *Member, IEEE,* Derrick Wing Kwan Ng, *Fellow, IEEE,*
Yonina C. Eldar, *Fellow, IEEE,* and Xiaohu You, *Fellow, IEEE*

Abstract—Beamforming design has been widely investigated for integrated sensing and communication (ISAC) systems with full-duplex (FD) sensing and half-duplex (HD) communication, where the base station (BS) transmits and receives radar sensing signals simultaneously while the integrated communication operates in either the downlink transmission or the uplink transmission. To achieve higher spectral efficiency, in this paper, we extend existing ISAC beamforming design to a general case by considering the FD capability for both radar and communication. Specifically, we consider an ISAC system, where the BS performs target detection and communicates with multiple downlink users and uplink users reusing the same time and frequency resources. We jointly optimize the downlink dual-functional transmit signal and the uplink receive beamformers at the BS and the transmit power at the uplink users. The problems are formulated under two criteria: power consumption minimization and sum rate maximization. The downlink and uplink transmissions are tightly coupled due to both the desired target echo and the undesired interference received at the BS, making the problems challenging. To handle these issues in both cases, we first determine the optimal receive beamformers, which are derived in closed forms with respect to the BS transmit beamforming and the user transmit power, for radar target detection and uplink communications, respectively. Subsequently, we invoke these results to obtain equivalent optimization problems and propose efficient iterative algorithms to solve them by using the techniques of rank relaxation and successive convex approximation (SCA), where the adopted relaxation is proven to be tight. In addition, we consider a special case under the power minimization criterion and propose an alternative low complexity design. Numerical results demonstrate that the optimized FD communication-based ISAC brings tremendous improvements in terms of both power efficiency and spectral efficiency compared to the conventional ISAC with HD communication, especially when the interference power is low and the sensing requirement is less restrictive.

Index Terms—Integrated sensing and communication (ISAC), full-duplex (FD) communication, joint transceiver optimization, beamforming design.

I. INTRODUCTION

With rapid development of commercial wireless communications, it is envisioned that an explosive number of intelligent

Zhenyao He, Wei Xu, Hong Shen, and Xiaohu You are with the National Mobile Communications Research Laboratory, Southeast University, Nanjing 210096, China (e-mail: {hezhenyao, wxu, shhseu, xhyu}@seu.edu.cn).

Derrick Wing Kwan Ng is with the School of Electrical Engineering and Telecommunications, University of New South Wales, Sydney, NSW 2052, Australia (e-mail: w.k.ng@unsw.edu.au).

Yonina C. Eldar is with the Faculty of Mathematics and Computer Science, Weizmann Institute of Science, Rehovot 76100, Israel (e-mail: yonina@weizmann.ac.il).

devices will be connected and will cooperate with each other in future networks. A consequent pressing problem is to satisfy the heterogeneous requirements of reliable sensing and efficient communication among these wireless terminals [2], [3]. On the other hand, the continuous and aggressive use of frequency spectrum in wireless communication systems, e.g., millimeter-wave (mmWave), results in overlapped spectrum with conventional radar systems. These motivate the development of frameworks for sensing-communication integration. In particular, integrated sensing and communication (ISAC), also known as dual-functional radar-communication or joint radar-communication, has become an appealing technique to address the aforementioned issues and has attracted considerable research interest. It has been shown in the literature [4]–[6] that ISAC can significantly enhance the spectral efficiency and reduce implemental cost by sharing spectral resources and reusing expensive hardware architectures. Also, joint design of communication and sensing can help improve the performances of both functionalities.

Effective transmit beamforming design is a key to unlock the potential in both multiple-input multiple-output (MIMO) communication systems and MIMO radar systems [7], [8]. Motivated by this, many works have studied transmit design in multi-antenna ISAC systems by focusing on joint beamforming optimization [9]–[13]. Specifically, for conventional MIMO radar systems, a commonly adopted strategy of probing signal design is to manipulate the transmit beampattern through optimizing the covariance matrix of the transmit signal, aiming to maximize the spatial power steered towards desired directions or to minimize the matching error between the transmit signal and a dedicated beampattern [7], [8]. Leveraging this strategy, the authors in [9] advocated the reuse of transmit signal for both multi-user communication and radar sensing in ISAC systems. Specifically, the beamforming was optimized by minimizing the beampattern matching error, taking into account individual signal-to-interference-plus-noise ratio (SINR) requirements of communication users. As an alternative, studies [10] and [11] considered similar problems while introducing a dedicated radar signal to facilitate the downlink ISAC. They introduced extra degrees-of-freedom (DoF) to the transmitted signal deliberately to achieve enhanced sensing accuracy. On the other hand, the authors of [11] investigated the problem of maximizing the transmit beampattern gain towards the sensing directions in ISAC, while guaranteeing the minimum required SINR of communication users. By imposing the constraint of transmit beampattern gain for sensing, the problems of communication

(a) Integrated sensing with downlink communication.
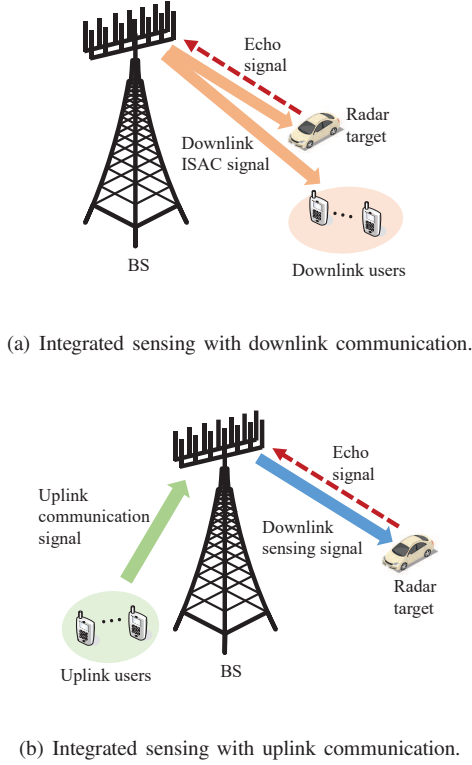

(b) Integrated sensing with uplink communication.

Fig. 1. Two cases of ISAC considered in [14]–[19]. (a) Integration of sensing with downlink communication: An ISAC signal is sent by the BS to perform simultaneous downlink communication and radar sensing, and the receive side of the BS remains active for the reception of radar echo; (b) Integration of sensing with uplink communication: The BS transmits a pure sensing signal and receives the echoes during the uplink communication.

spectral efficiency maximization [12] and energy efficiency maximization [13] were addressed for ISAC. Note that these works only design the transmit beamforming while the reception of radar echo is not considered.

The main function of a radar system is to estimate the channel parameters, e.g., delay and Doppler frequency, of a target from the received radar echo signal. With the consideration of radar echo reception in ISAC systems, e.g., [14]–[19], the associated scenarios are divided into two cases, as illustrated in Fig. 1. The first case in Fig. 1(a) corresponds to downlink ISAC [14]–[17], where the radar sensing reuses the resources of downlink transmission and the BS acts as a radar transceiver and a communication transmitter. The transmitted downlink ISAC signal is known to the BS and can be used in receive processing for sensing. In this case, the authors of [14] investigated the Cramér-Rao bound (CRB) minimization of target parameter estimation for ISAC. In [15]–[17], the authors considered the tasks of point target detection in ISAC systems. In these works, they acquired explicitly the radar SINR for target detection by applying a linear receive beamformer to the echo signal. More concretely, given a fixed radar receive beamformer, the optimizations of the transmit signals were investigated in [15] and [16], where a minimal radar SINR requirement for accomplishing the target detection is constrained. In [17], an alternating optimization (AO)-based algorithm was proposed to iteratively update the transmit

waveform and the radar receive beamformer. The second scenario in Fig. 1(b) considers integrating sensing with uplink communication [18], [19], where the BS can be regarded as a radar transceiver and a communication receiver. The authors of [18] developed an advanced receiver architecture for uplink ISAC, which separates the radar echo and communication signals by performing interference cancellation techniques. Sensing-assisted physical-layer security transmission was investigated in [19], where the BS transmits a downlink radar signal to localize and jam a potential aerial eavesdropper while receiving the uplink communication signal.

In the aforementioned works [14]–[19], the radar receiver operates simultaneously while transmitting, i.e., in a full-duplex (FD) manner, especially for short-range radar. Self-interference (SI), which is a critical issue in FD operation, is considered to be significantly suppressed by installing spatially widely-separated transmit and receive antennas and employing advanced SI cancellation techniques [5], [18], [20], [21]. Particularly, in an FD ISAC system, the SI cancellation should be performed for the direct coupling between the transceiver antennas only, while target reflections should be preserved [20]. With FD radar, however, the integrated communication functionality occurs only in either the downlink or the uplink, operating in a half-duplex (HD) manner [14]–[19]. Therefore, it is natural to consider the FD capability also for communication to achieve higher spectral efficiency [22], i.e., to let the BS serve as both a radar transceiver and a communication transceiver concurrently. Under this setup, there is not only interference between sensing and communication functionalities, but also coupling between uplink and downlink transmissions, that significantly complicate the ISAC design. Existing algorithms in [14]–[19] cannot be straightforwardly applied to address these challenges. Specifically, the algorithms designed in [14]–[17] do not incorporate the impact of uplink communication. In [18], [19], only a pure downlink sensing signal is sent and the uplink transmit power is fixed, without considering the possibility of downlink communication nor designing the uplink transmission.

Motivated by the above discussion, we investigate an advanced FD communication-based ISAC system, where the BS receives and transmits signals from multiple uplink users and downlink users reusing the same time and frequency resources. The downlink transmit signal is an ISAC signal that is applied for both conveying information to the downlink users and performing a sensing task of point target detection. The BS also simultaneously conducts uplink communication signals reception and processes the radar echo signal. Our goal is to jointly design the transceiver beamforming at the FD BS and the transmit power at the single-antenna uplink users. In the considered FD system, the SI at the BS, or more precisely, the direct coupling link between the transceiver, is assumed to be suppressed to an acceptable level by employing SI cancellation techniques for ISAC systems [18], [21]. The received signals at the BS consist of uplink communication signals, desired target reflection, and downlink signal-dependent interference from environmental interferers and residual SI.

To detect both the sensing target and multiuser uplink signals with low complexity, multiple linear receive beamformers

are employed at the BS and the corresponding radar and uplink communication SINRs are mathematically obtained. As such, we formulate two different fundamental problems for the joint optimization. The first problem focuses on power minimization by constraining the minimal SINR requirements of target detection, uplink communications, and downlink communications. The second problem aims at maximizing the sum rate of the FD multiuser communication, subject to the constraint of minimal sensing SINR requirement and the limit of maximal transmit powers. Compared to [14]–[19], we consider the joint optimization for both uplink and downlink transmissions of the FD ISAC system, which are highly coupled and intractable. The main contributions of this paper are summarized as follows:

- We extend existing ISAC beamforming design to a general case by considering the FD capability for both radar and communication and focusing on the optimization of the coupled downlink and uplink transmissions. With the employment of linear receive beamformers, the SINRs of radar sensing and communication of the FD ISAC system are mathematically formulated and two different problems are constructed aiming to improve the system power efficiency and spectral efficiency, respectively.
- We derive the optimal receive beamformers to maximize the SINR of target detection and the SINRs of uplink communication, respectively, which are obtained as closed-form expressions with respect to the BS transmit beamforming and the user transmit power.
- For each of the two considered problems, we first obtain an equivalent problem that involves the optimization of only the BS transmit beamforming and the user transmit power based on the closed-form receivers. Subsequently, an iterative algorithm is proposed to find a high-quality solution by applying the techniques of rank relaxation and successive convex approximation (SCA). We prove that the adopted relaxation is tight.
- For the problem of power minimization, we further consider a special case of HD uplink communication-based ISAC in the absence of downlink users, while the downlink signal is adopted for target detection only. Instead of applying the SCA-based algorithm as in the general case, we propose an AO-based algorithm to iteratively update the receive beamformers and the other variables, whose solutions are obtained by calculating closed-form expressions and by solving a second-order cone programming (SOCP), respectively. Numerical results verify that this newly proposed method significantly reduces the computational complexity compared to the SCA-based method with almost the same performance.

The rest of this paper is organized as follows. In Section II, we present the model of the considered FD ISAC system and the formulation of the power minimization and sum rate maximization problems. Section III and Section IV provide detailed solutions to these two problems, respectively. In Section V, we verify the effectiveness of the proposed algorithms through numerical simulations. Conclusions are drawn in Section IV.
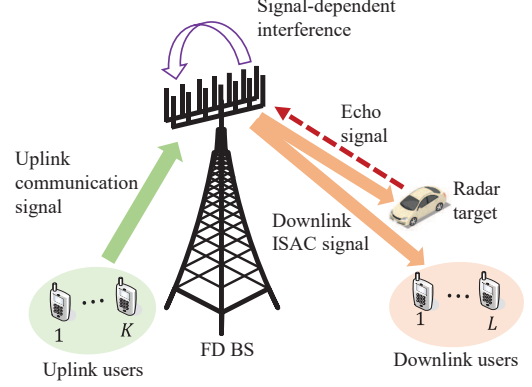
Notations: Boldface lower-case and boldface upper-case

Fig. 2. The considered FD communication-based ISAC system with K uplink users, L downlink users, and a point radar target.

letters are used to represent vectors and matrices, respectively. Denote superscripts $(\cdot)^T$ and $(\cdot)^H$ by the transpose and the Hermitian transpose, respectively. Let $\text{Tr}(\cdot)$, $\text{rank}(\cdot)$, and $[\cdot]_{i,j}$ return the trace, the rank, and the (i,j)-th entry of a matrix, respectively. Denote $\|\cdot\|$ by the ℓ_2 norm of a vector and $|\cdot|$ by the absolute value of a scalar. We use $\mathbb{E}\{\cdot\}$ for the expectation operation, $\mathcal{I}\{\cdot\}$ for the imaginary part of a complex-valued number, $\mathbb{C}$ for the set of complex-value numbers, and $\mathbf{I}_N$ for the identity matrix of size $N \times N$. Let $\mathbf{X} \succeq \mathbf{0}$ imply that $\mathbf{X}$ is positive semidefinite. Denote $\mathcal{O}(\cdot)$ by the big-O computational complexity notation.

II. System Model and Problem Formulation

Consider an ISAC system as shown in Fig. 2, where a dual-functional FD BS equipped with two uniform linear arrays (ULAs) receives the communication signals from K single-antenna uplink users and sends a downlink ISAC signal via the same time-frequency resource. The downlink ISAC signal transmitted from an N_t-element ULA is adopted for simultaneously communicating with L single-antenna downlink users and performing target detection on a point radar target. The radar echo signal and the uplink communication signals are received at the BS through the receive ULA with N_r elements.

A. Signal Model

We first focus on the downlink transmission of the system, where an ISAC signal, $\mathbf{x} \in \mathbb{C}^{N_t \times 1}$, is sent for simultaneous radar sensing and downlink multiuser communication via multi-antenna beamforming. Following [10]–[14], the integrated signal is expressed as

$$\mathbf{x} = \sum_{l=1}^{L} \mathbf{v}_l s_l + \mathbf{s}_0, \qquad (1)$$

where $\mathbf{v}_l \in \mathbb{C}^{N_t \times 1}$ stands for the beamforming vector associated with downlink user l, $l \in \{1, \cdots, L\}$, and $s_l \in \mathbb{C}$ is the data symbol of user l with unit power, i.e., $\mathbb{E}\{|s_l|^2\} = 1$. Here, $\mathbf{s}_0 \in \mathbb{C}^{N_t \times 1}$ represents a dedicated radar signal with

covariance matrix $\mathbf{V}_0 \triangleq \mathbb{E}\{\mathbf{s}_0\mathbf{s}_0^H\}$. The signals $\{s_l\}_{l=1}^L$ and $\mathbf{s}_0$ are assumed to be independent with each other. In (1), the downlink beamforming is achieved by designing $\{\mathbf{v}_l\}_{l=1}^L$ and $\mathbf{V}_0$ [10]–[14]. Once $\mathbf{V}_0$ is determined, the dedicated radar signal $\mathbf{s}_0$ can be generated [8]. Moreover, we consider a total transmit power constraint as $\sum_{l=1}^L \|\mathbf{v}_l\|^2 + \text{Tr}(\mathbf{V}_0) \leq P_{\max}$, where $P_{\max}$ denotes the maximum available power budget of the BS.

When the FD BS transmits $\mathbf{x}$, it simultaneously receives the uplink communication signals and the target reflection. Let $d_k \in \mathbb{C}$ denote the uplink signal from user k, $k \in \{1, \cdots, K\}$, which satisfies

$$\mathbb{E}\{|d_k|^2\} = p_k, \ \forall k, \tag{2}$$

where $0 \leq p_k \leq P_k$ represents the average transmit power of user k with P_k being the maximum power budget. Denoting the uplink channel between the k-th user and the BS by $\mathbf{h}_k \in \mathbb{C}^{N_r \times 1}$, the received multiuser uplink signal at the BS is $\sum_{k=1}^K \mathbf{h}_k d_k$. The design of uplink transmission is achieved by adjusting the transmit power $\{p_k\}_{k=1}^K$ of uplink users.

We next model the echo signal reflected by the target. Assume that the radar channel consists of line-of-sight paths. Let $\mathbf{a}_t(\theta) \triangleq \frac{1}{\sqrt{N_t}}\left[1, e^{j2\pi\frac{d}{\lambda}\sin(\theta)}, \cdots, e^{j2\pi\frac{d}{\lambda}(N_t-1)\sin(\theta)}\right]^T$ stand for the transmit array steering vector of direction θ at the BS, where d denotes the spacing between two adjacent antennas, and λ is the carrier wavelength. We similarly define $\mathbf{a}_r(\theta) \triangleq \frac{1}{\sqrt{N_r}}\left[1, e^{j2\pi\frac{d}{\lambda}\sin(\theta)}, \cdots, e^{j2\pi\frac{d}{\lambda}(N_r-1)\sin(\theta)}\right]^T$ as the receive steering vector. Supposing that the target to be detected is located at angle θ_0, the target reflection is given by $\beta_0\mathbf{a}_r(\theta_0)\mathbf{a}_t^H(\theta_0)\mathbf{x}$, where $\beta_0 \in \mathbb{C}$ is the complex amplitude of the target mainly determined by the path loss and the radar cross-section [15]. Assume that θ_0 and β_0 are known to the BS for designing the best suitable transmit signal to detect this specific target of interest [23]. Based on the given uplink communication signal and the target echo, we express the received signal at the FD BS as

$$\mathbf{y}^{\text{BS}} = \sum_{k=1}^K \mathbf{h}_k d_k + \beta_0\mathbf{A}(\theta_0)\mathbf{x} + \mathbf{z} + \mathbf{n}, \tag{3}$$

where $\mathbf{A}(\theta_0) \triangleq \mathbf{a}_r(\theta_0)\mathbf{a}_t^H(\theta_0)$, $\mathbf{n} \in \mathbb{C}^{N_r \times 1}$ stands for additive white Gaussian noise (AWGN) at the receive array with covariance $\sigma_r^2\mathbf{I}_{N_r}$, and $\mathbf{z} \in \mathbb{C}^{N_r \times 1}$ represents the undesired signal-dependent interference which is detailed in the next paragraph.

The signal-dependent interference $\mathbf{z}$ can be decomposed into two parts. The first part corresponds to the clutter reflected from the surrounding environment. Without loss of generality, we follow [17], [24] and assume that there exist I signal-dependent uncorrelated interferers located at angles $\{\theta_i\}_{i=1}^I$ and $\theta_i \neq \theta_0$, $\forall i \in \{1, \cdots, I\}$. These I interferers also reflect the sensing signal to the BS, yielding the undesired interference $\sum_{i=1}^I \beta_i\mathbf{A}(\theta_i)\mathbf{x}$ with $\beta_i \in \mathbb{C}$ being the complex amplitude of the i-th interferer and $\mathbf{A}(\theta_i) \triangleq \mathbf{a}_r(\theta_i)\mathbf{a}_t^H(\theta_i)$, $\forall i$. The second part is the residual SI after employing the SI cancellation techniques for ISAC systems [18], [21]. According to [18], we express the SI signal as $\mathbf{H}_{\text{SI}}\mathbf{x}$, where $\mathbf{H}_{\text{SI}} \in \mathbb{C}^{N_r \times N_t}$

denotes the residual SI channel at the FD BS and it is modeled as $\mathbf{H}_{\text{SI}} = \sqrt{\alpha_{\text{SI}}}\tilde{\mathbf{H}}_{\text{SI}}$. Here, $\alpha_{\text{SI}} > 0$ stands for the residual SI channel power and each entry of $\tilde{\mathbf{H}}_{\text{SI}} \in \mathbb{C}^{N_r \times N_t}$ is modeled as $[\tilde{\mathbf{H}}_{\text{SI}}]_{p,q} = e^{-j2\pi\frac{d_{p,q}}{\lambda}}$ with $d_{p,q} > 0$ denoting the distance between the q-th transmit antenna and the p-th receive antenna. Combining the two parts of interference, $\mathbf{z}$ is expressed as

$$\mathbf{z} = \sum_{i=1}^I \beta_i\mathbf{A}(\theta_i)\mathbf{x} + \mathbf{H}_{\text{SI}}\mathbf{x}. \tag{4}$$

By substituting (4) into (3), we express the complete received signal at the FD BS as

$$\mathbf{y}^{\text{BS}} = \underbrace{\sum_{k=1}^K \mathbf{h}_k d_k}_{\text{Communication signal}} + \underbrace{\beta_0\mathbf{A}(\theta_0)\mathbf{x}}_{\text{Target reflection}} + \underbrace{\sum_{i=1}^I \beta_i\mathbf{A}(\theta_i)\mathbf{x}}_{\text{Echo signal of interferers}} + \underbrace{\mathbf{H}_{\text{SI}}\mathbf{x}}_{\text{SI}} + \mathbf{n}. \tag{5}$$

On the other hand, denote the channel between downlink user l and the BS by $\mathbf{g}_l \in \mathbb{C}^{N_t \times 1}$. The received signal at downlink user l is then expressed as

$$y_l^{\text{User}} = \underbrace{\mathbf{g}_l^H\mathbf{v}_l s_l}_{\text{Desired signal}} + \underbrace{\sum_{l'=1,l'\neq l}^L \mathbf{g}_l^H\mathbf{v}_{l'}s_{l'}}_{\text{Multiuser interference}} + \underbrace{\mathbf{g}_l^H\mathbf{s}_0}_{\text{Sensing signal}} + n_l, \ \forall l, \tag{6}$$

where n_l stands for the AWGN with variance σ_l^2. Although a few prior works on the uplink ISAC, e.g., [18], [19], also considered a similar received signal model at the ISAC BS as (5), this paper is noticeably different from these works in terms of the following two aspects. First, the downlink transmitted $\mathbf{x}$ in our system is a dual-functional ISAC signal that serves both communication and sensing, while only a pure radar signal was sent in [18], [19]. Second, studies [18], [19] mainly focused on the receiver design with a fixed uplink transmit power without adaptability. To enable more design flexibility and gain further performance improvements, in this paper, we additionally introduce the optimization of the uplink transmission, i.e., $\{p_k\}_{k=1}^K$.

Before proceeding, we would like to clarify some assumptions employed in the considered system. First in (3), the angles of a target seen at the transceiver are identical, which is a reasonable assumption when the transmit array and the receive array are collocated [7]. Second, it is assumed that $\{\theta_i\}_{i=1}^I$ and $\{|\beta_i|^2\}_{i=1}^I$ in (4) can be pre-estimated and known to the ISAC system for transceiver design [17] by using an environmental dynamic database [24]. Finally, we assume that a dedicated channel estimation stage is utilized before the FD transmission such that the channel state information is available at the BS for beamforming design [18].

B. Radar and Communication SINR

The performances of the radar and the communication systems largely depend on the corresponding SINRs. In particular, when considering point target detection in MIMO radar systems, the detection probability of a target is generally a monotonically increasing function of the output SINR [25]. Therefore, we directly adopt radar SINR as the performance

metric of the sensing functionality. Technically, we apply a receive beamformer $\mathbf{u} \in \mathbb{C}^{N_r \times 1}$ on the received signal, $\mathbf{y}^{\text{BS}}$, to capture the desired reflected signal of the point target. Then, based on (5), we obtain the radar SINR as

$$\gamma^{\text{rad}} = \frac{\mathbb{E}\{|\mathbf{u}^H \beta_0 \mathbf{A}(\theta_0)\mathbf{x}|^2\}}{\sum_{k=1}^K \mathbb{E}\{|\mathbf{u}^H \mathbf{h}_k d_k|^2\} + \mathbb{E}\{|\mathbf{u}^H \mathbf{B}\mathbf{x}|^2\} + \mathbb{E}\{|\mathbf{u}^H \mathbf{n}|^2\}}$$

$$= \frac{|\beta_0|^2 \mathbf{u}^H \mathbf{A}(\theta_0)\mathbf{Q}\mathbf{A}(\theta_0)^H \mathbf{u}}{\mathbf{u}^H \left(\sum_{k=1}^K p_k \mathbf{h}_k \mathbf{h}_k^H + \mathbf{B}\mathbf{Q}\mathbf{B}^H + \sigma_r^2 \mathbf{I}_{N_r}\right) \mathbf{u}}, \quad (7)$$

where $\mathbf{B} \triangleq \sum_{i=1}^I \beta_i \mathbf{A}(\theta_i) + \mathbf{H}_{\text{SI}}$ represents the interference channel defined as the summation of the I interferers' channels and the SI channel, and

$$\mathbf{Q} \triangleq \mathbb{E}\{\mathbf{x}\mathbf{x}^H\} = \sum_{l=1}^L \mathbf{v}_l \mathbf{v}_l^H + \mathbf{V}_0 \quad (8)$$

denotes the covariance matrix of the downlink ISAC signal that needs to be well designed. Note that the radar SINR was employed as a sensing metric for beamforming design in ISAC before, but only under the downlink scenario in the absence of uplink communication, e.g., [15]–[17]. The term $\sum_{k=1}^K p_k \mathbf{h}_k \mathbf{h}_k^H + \mathbf{B}\mathbf{Q}\mathbf{B}^H$ makes the radar SINR expression in (7) in our considered FD ISAC more complicated than those in [15]–[17], as it introduces signal-dependent interference and coupled uplink transmission.

Similarly, by applying another set of receive beamformers $\{\mathbf{w}_k\}_{k=1}^K \in \mathbb{C}^{N_r \times 1}$ on $\mathbf{y}^{\text{BS}}$ to recover the data signals of the uplink users, we obtain the corresponding receive SINR of user k by

$$\gamma_k^{\text{com,UL}} = \frac{p_k \mathbf{w}_k^H \mathbf{h}_k \mathbf{h}_k^H \mathbf{w}_k}{\mathbf{w}_k^H \left(\sum_{k'=1, k' \neq k}^K p_{k'} \mathbf{h}_{k'} \mathbf{h}_{k'}^H + \mathbf{C}\mathbf{Q}\mathbf{C}^H + \sigma_r^2 \mathbf{I}_{N_r}\right) \mathbf{w}_k}, \quad \forall k, \quad (9)$$

where $\mathbf{C} \triangleq \sum_{i=0}^I \beta_i \mathbf{A}(\theta_i) + \mathbf{H}_{\text{SI}}$ denotes the interference channel caused by the downlink transmission. As for the downlink communication, it follows from (6) that the SINR of the downlink user l is given by[1]

$$\gamma_l^{\text{com,DL}} = \frac{|\mathbf{g}_l^H \mathbf{v}_l|^2}{\sum_{l'=1, l' \neq l}^L |\mathbf{g}_l^H \mathbf{v}_{l'}|^2 + \mathbf{g}_l^H \mathbf{V}_0 \mathbf{g}_l + \sigma_l^2}, \quad \forall l. \quad (10)$$

C. Problem Formulation

We aim at jointly optimizing the transmit power, $\{p_k\}_{k=1}^K$, at the uplink users, the receive beamformers, $\{\mathbf{w}_k\}_{k=1}^K$ and $\mathbf{u}$, and the transmit beamforming, $\{\mathbf{v}_l\}_{l=1}^L$ and $\mathbf{V}_0$, at the BS for the considered FD ISAC system. Denote $\mathcal{A} \triangleq \left\{\{\mathbf{w}_k\}_{k=1}^K, \mathbf{u}, \{\mathbf{v}_l\}_{l=1}^L, \mathbf{V}_0 \succeq \mathbf{0}, \{p_k\}_{k=1}^K\right\}$ as the set of optimization variables. The joint design is performed under two criteria: 1) transmit power minimization; 2) overall sum rate maximization, which correspond to the power efficiency and the spectral efficiency improvement of the ISAC system, respectively. Specifically, for the first design criterion, we consider minimizing the total transmit power consumption while guaranteeing the minimal SINR requirements of uplink

---

[1]Here, we consider the users which are not capable of canceling the interference of the dedicated radar signal $\mathbf{s}_0$ [11].

communications, downlink communications, and radar sensing. The corresponding problem is formulated as

$$\underset{\mathcal{A}}{\text{minimize}} \quad \sum_{l=1}^L \|\mathbf{v}_l\|^2 + \text{Tr}(\mathbf{V}_0) + \sum_{k=1}^K p_k$$

$$\text{subject to} \quad \gamma^{\text{rad}} \geq \tau^{\text{rad}},$$
$$\gamma_k^{\text{com,UL}} \geq \tau_k^{\text{com,UL}}, \ \forall k,$$
$$\gamma_l^{\text{com,DL}} \geq \tau_l^{\text{com,DL}}, \ \forall l, \quad (11)$$

where τ^{rad} is the required constant minimal SINR threshold for successfully accomplishing the sensing operation, and $\tau_k^{\text{com,UL}}$ and $\tau_l^{\text{com,DL}}$ stand for the minimal SINR requirements of uplink user k and downlink user l, respectively.

We also wish to maximize the sum rate of all the uplink and downlink users with limited transmit power budgets, while guaranteeing the sensing performance by constraining the minimal required radar SINR. Accordingly, we formulate the problem as

$$\underset{\mathcal{A}}{\text{maximize}} \quad \sum_{k=1}^K \log_2(1 + \gamma_k^{\text{com,UL}}) + \sum_{l=1}^L \log_2(1 + \gamma_l^{\text{com,DL}})$$

$$\text{subject to} \quad \gamma^{\text{rad}} \geq \tau^{\text{rad}},$$

$$\sum_{l=1}^L \|\mathbf{v}_l\|^2 + \text{Tr}(\mathbf{V}_0) \leq P_{\text{max}},$$

$$p_k \leq P_k, \ \forall k. \quad (12)$$

Observe that both (11) and (12) are nonconvex problems whose globally optimal solutions are hard to obtain by polynomial-time algorithms in general. Moreover, the optimization variables are tightly coupled which further complicates the problems and makes them intractable. In the following sections, we propose efficient algorithms to solve these two problems, respectively.

III. JOINT FD ISAC DESIGN FOR POWER MINIMIZATION

We handle (11) in this section. Specifically, we first determine the optimal receive beamformers $\{\{\mathbf{w}_k\}_{k=1}^K, \mathbf{u}\}$ in closed-form expressions with respect to $\{\{\mathbf{v}_l\}_{l=1}^L, \mathbf{V}_0, \{p_k\}_{k=1}^K\}$ and substitute them into (11). Then, we address the equivalent problem exploiting the SCA technique. In addition, we investigate a special case and provide a low-complexity solution.

A. Closed-Form Solutions to Receive Beamformer

Note that the objective of (11) does not depend on $\{\{\mathbf{w}_k\}_{k=1}^K, \mathbf{u}\}$. Moreover, given arbitrary feasible $\{\{\mathbf{v}_l\}_{l=1}^L, \mathbf{V}_0, \{p_k\}_{k=1}^K\}$, it can be found that $\mathbf{u}$ only affects the value of γ^{rad} and $\mathbf{w}_k$ has an impact on $\gamma_k^{\text{com,UL}}$ while it does not affect the SINRs of other users. Therefore, to facilitate the fulfillment of the SINR constraints in (11) and reduce the transmit power consumption, the receive beamformers $\{\{\mathbf{w}_k\}_{k=1}^K, \mathbf{u}\}$ should be determined by maximizing the

corresponding SINRs. As a result, we optimize $\{\mathbf{w}_k\}_{k=1}^{K}$ and $\mathbf{u}$ through the SINR maximization criterion:

$$\underset{\mathbf{u}}{\text{maximize}} \quad \gamma^{\text{rad}}, \tag{13}$$

$$\underset{\mathbf{w}_k}{\text{maximize}} \quad \gamma_k^{\text{com,UL}}, \ \forall k. \tag{14}$$

Proposition 1: The optimal solutions to (13) and (14) are given by

$$\mathbf{u}^* = \left(\sum_{k=1}^{K} p_k \mathbf{h}_k \mathbf{h}_k^H + \mathbf{BQB}^H + \sigma_r^2 \mathbf{I}_{N_r} \right)^{-1} \mathbf{a}_r(\theta_0), \tag{15}$$

$$\mathbf{w}_k^* = \left(\sum_{k'=1,k'\neq k}^{K} p_{k'} \mathbf{h}_{k'} \mathbf{h}_{k'}^H + \mathbf{CQC}^H + \sigma_r^2 \mathbf{I}_{N_r} \right)^{-1} \mathbf{h}_k, \ \forall k, \tag{16}$$

respectively, which rely on the transmit beamforming at the BS and the transmit powers of uplink users.

Proof: See Appendix A. ∎

Note that scaling $\mathbf{u}^*$ and $\mathbf{w}_k^*$, $\forall k$, with any positive constant does not affect the optimality.

B. Solutions to Transmit Beamforming and Power

Substituting the optimal $\{\{\mathbf{w}_k^*\}_{k=1}^{K}, \mathbf{u}^*\}$ into the SINR expressions in (7) and (9) yields

$$\bar{\gamma}^{\text{rad}} = |\beta_0|^2 \mathbf{a}_t^H(\theta_0) \mathbf{Q} \mathbf{a}_t(\theta_0)$$
$$\times \mathbf{a}_r^H(\theta_0) \left(\sum_{k=1}^{K} p_k \mathbf{h}_k \mathbf{h}_k^H + \mathbf{BQB}^H + \sigma_r^2 \mathbf{I}_{N_r} \right)^{-1} \mathbf{a}_r(\theta_0), \tag{17}$$

$$\bar{\gamma}_k^{\text{com,UL}} = p_k \mathbf{h}_k^H \left(\sum_{k'=1,k'\neq k}^{K} p_{k'} \mathbf{h}_{k'} \mathbf{h}_{k'}^H + \mathbf{CQC}^H + \sigma_r^2 \mathbf{I}_{N_r} \right)^{-1} \mathbf{h}_k, \ \forall k, \tag{18}$$

respectively. Subsequently, applying (17) and (18), we rewrite (11) into the following equivalent problem with respect to $\{\{\mathbf{v}_l\}_{l=1}^{L}, \mathbf{V}_0, \{p_k\}_{k=1}^{K}\}$:

$$\underset{\substack{\{\mathbf{v}_l\}_{l=1}^{L}, \mathbf{V}_0 \succeq \mathbf{o}, \\ \{p_k \geq 0\}_{k=1}^{K}}}{\text{minimize}} \quad \sum_{l=1}^{L} \|\mathbf{v}_l\|^2 + \text{Tr}(\mathbf{V}_0) + \sum_{k=1}^{K} p_k$$

$$\text{subject to} \quad \bar{\gamma}^{\text{rad}} \geq \tau^{\text{rad}},$$
$$\bar{\gamma}_k^{\text{com,UL}} \geq \tau_k^{\text{com,UL}}, \ \forall k,$$
$$\gamma_l^{\text{com,DL}} \geq \tau_l^{\text{com,DL}}, \ \forall l. \tag{19}$$

The above problem is still nonconvex due to the complicated SINR constraints. To handle this issue, we introduce a set of auxiliary variables $\mathbf{V}_l \triangleq \mathbf{v}_l \mathbf{v}_l^H$, $\forall l$. With $\{\mathbf{V}_l\}_{l=1}^{L}$, we further define $\bar{\mathbf{Q}} \triangleq \sum_{l=0}^{L} \mathbf{V}_l$, $\mathbf{\Psi} \triangleq \sum_{k=1}^{K} p_k \mathbf{h}_k \mathbf{h}_k^H + \mathbf{B}\bar{\mathbf{Q}}\mathbf{B}^H + \sigma_r^2 \mathbf{I}_{N_r}$, and $\mathbf{\Phi}_k \triangleq \sum_{k'=1,k'\neq k}^{K} p_{k'} \mathbf{h}_{k'} \mathbf{h}_{k'}^H + \mathbf{C}\bar{\mathbf{Q}}\mathbf{C}^H + \sigma_r^2 \mathbf{I}_{N_r}$, $\forall k$,

to simplify the SINR expressions. After some straightforward algebraic operations, (19) is recast as

$$\underset{\substack{\{\mathbf{V}_l \succeq \mathbf{o}\}_{l=0}^{L}, \\ \{p_k \geq 0\}_{k=1}^{K}}}{\text{minimize}} \quad \sum_{l=0}^{L} \text{Tr}(\mathbf{V}_l) + \sum_{k=1}^{K} p_k \tag{20}$$

$$\text{subject to} \quad \mathbf{a}_t^H(\theta_0)\bar{\mathbf{Q}}\mathbf{a}_t(\theta_0)\mathbf{a}_r^H(\theta_0)\mathbf{\Psi}^{-1}\mathbf{a}_r(\theta_0) \geq \frac{\tau^{\text{rad}}}{|\beta_0|^2}, \tag{20a}$$

$$\mathbf{h}_k^H \mathbf{\Phi}_k^{-1} \mathbf{h}_k \geq \frac{\tau_k^{\text{com,UL}}}{p_k}, \ \forall k, \tag{20b}$$

$$\left(1 + \frac{1}{\tau_l^{\text{com,DL}}}\right) \mathbf{g}_l^H \mathbf{V}_l \mathbf{g}_l \geq \mathbf{g}_l^H \bar{\mathbf{Q}} \mathbf{g}_l + \sigma_l^2,$$
$$\forall l \geq 1. \tag{20c}$$

Note that we omitted the rank constraints of $\{\mathbf{V}_l\}_{l=1}^{L}$, i.e.,

$$\text{rank}(\mathbf{V}_l) \leq 1, \ \forall l \geq 1, \tag{21}$$

based on the idea of rank relaxation [26]. The reformulation in (20) still has nonconvex constraints (20a) and (20b).

To obtain a more tractable form, we employ the iterative SCA technique to handle constraints (20a) and (20b). Focusing on (20a), due to the fact that $\{\mathbf{V}_l \succeq \mathbf{0}\}_{l=0}^{L}$, we have $\bar{\mathbf{Q}} \succeq \mathbf{0}$ and $\mathbf{a}_t^H(\theta_0)\bar{\mathbf{Q}}\mathbf{a}_t(\theta_0) \geq 0$. Moreover, it must hold that $\mathbf{a}_t^H(\theta_0)\bar{\mathbf{Q}}\mathbf{a}_t(\theta_0) \neq 0$ since the radar SINR threshold $\tau^{\text{rad}} > 0$. Thus, by dividing both sides of (20a) by $\mathbf{a}_t^H(\theta_0)\bar{\mathbf{Q}}\mathbf{a}_t(\theta_0)$, it becomes

$$\mathbf{a}_r^H(\theta_0)\mathbf{\Psi}^{-1}\mathbf{a}_r(\theta_0) \geq \frac{\tau^{\text{rad}}}{|\beta_0|^2} \left(\mathbf{a}_t^H(\theta_0)\bar{\mathbf{Q}}\mathbf{a}_t(\theta_0)\right)^{-1}. \tag{22}$$

Considering that the function $f(\mathbf{Y}) = \mathbf{f}^H \mathbf{Y}^{-1} \mathbf{f}$ is convex with respect to $\mathbf{Y}$ for $\mathbf{Y} \succ \mathbf{0}$ [27, Section 3.1.7] and $\mathbf{\Psi}$ is an affine function of $\{\{\mathbf{V}_l\}_{l=0}^{L}, \{p_k\}_{k=1}^{K}\}$, the left-hand side of (22) is convex with respect to $\mathbf{\Psi}$, and is also convex with respect to $\{\{\mathbf{V}_l\}_{l=0}^{L}, \{p_k\}_{k=1}^{K}\}$ [27, Section 3.2.2]. Similarly, the right-hand side of (22) is convex with respect to $\{\mathbf{V}_l\}_{l=0}^{L}$. Therefore, (22) is a difference-of-convex (DC) constraint which can be handled by iteratively lower bounding the left-hand side by its first-order Taylor expansion [28]. Specifically, according to the complex-valued derivatives in [29], for the i-th iteration of the SCA, we consider the following lower bound:

$$\mathbf{a}_r^H(\theta_0)\mathbf{\Psi}^{-1}\mathbf{a}_r(\theta_0)$$
$$\geq \mathbf{a}_r^H(\theta_0)\left(\mathbf{\Psi}^{(i-1)}\right)^{-1}\mathbf{a}_r(\theta_0) - \mathbf{a}_r^H(\theta_0)\left(\mathbf{\Psi}^{(i-1)}\right)^{-1}$$
$$\times \left(\mathbf{\Psi} - \mathbf{\Psi}^{(i-1)}\right)\left(\mathbf{\Psi}^{(i-1)}\right)^{-1}\mathbf{a}_r(\theta_0)$$
$$\triangleq f\left(\mathbf{\Psi}, \mathbf{\Psi}^{(i-1)}\right), \tag{23}$$

where $\mathbf{\Psi}^{(i-1)} \triangleq \sum_{k=1}^{K} p_k^{(i-1)} \mathbf{h}_k \mathbf{h}_k^H + \mathbf{B}\bar{\mathbf{Q}}^{(i-1)}\mathbf{B}^H + \sigma_r^2 \mathbf{I}_{N_r}$ and $\bar{\mathbf{Q}}^{(i-1)} = \sum_{l=0}^{L} \mathbf{V}_l^{(i-1)}$ with $\{p_k^{(i-1)}\}_{k=1}^{K}$ and $\{\mathbf{V}_l^{(i-1)}\}_{l=0}^{L}$ being the solutions obtained in the $(i-1)$-th iteration. As such, a convex subset of the nonconvex constraint in (20a) is established as

$$f\left(\mathbf{\Psi}, \mathbf{\Psi}^{(i-1)}\right) \geq \frac{\tau^{\text{rad}}}{|\beta_0|^2} \left(\mathbf{a}_t^H(\theta_0)\bar{\mathbf{Q}}\mathbf{a}_t(\theta_0)\right)^{-1}. \tag{24}$$

Next, we consider the constraints in (20b). For each k, it can be similarly verified that $\mathbf{h}_k^H \boldsymbol{\Phi}_k^{-1} \mathbf{h}_k$ is convex with respect to $\boldsymbol{\Phi}_k$ and we thus exploit its first-order Taylor expansion to obtain an affine approximation as

$$
\mathbf{h}_k^H \boldsymbol{\Phi}_k^{-1} \mathbf{h}_k \geq \mathbf{h}_k^H \left(\boldsymbol{\Phi}_k^{(i-1)} \right)^{-1} \mathbf{h}_k - \mathbf{h}_k^H \left(\boldsymbol{\Phi}_k^{(i-1)} \right)^{-1}
$$
$$
\times \left(\boldsymbol{\Phi}_k - \boldsymbol{\Phi}_k^{(i-1)} \right) \left(\boldsymbol{\Phi}_k^{(i-1)} \right)^{-1} \mathbf{h}_k
$$
$$
\triangleq f\left(\boldsymbol{\Phi}_k, \boldsymbol{\Phi}_k^{(i-1)} \right), \ \forall k, \tag{25}
$$

where $\boldsymbol{\Phi}_k^{(i-1)} \triangleq \sum_{k'=1, k' \neq k}^{K} p_{k'}^{(i-1)} \mathbf{h}_{k'} \mathbf{h}_{k'}^H + \mathbf{C} \bar{\mathbf{Q}}^{(i-1)} \mathbf{C}^H + \sigma_r^2 \mathbf{I}_{N_r}$ is calculated based on the solutions obtained in the $(i-1)$-th iteration. With (25), a convex subset of (20b) is given by

$$
f\left(\boldsymbol{\Phi}_k, \boldsymbol{\Phi}_k^{(i-1)} \right) \geq \frac{\tau_k^{\text{com,UL}}}{p_k}, \ \forall k. \tag{26}
$$

Based on the convex approximations in (23) and (25), we are ready to obtain a series of surrogate problems to locally approximate (20). Specifically, the surrogate problem in the i-th iteration is formulated as

$$
\begin{aligned}
& \underset{\substack{\{\mathbf{V}_l \succeq \mathbf{0}\}_{l=0}^{L}, \\ \{p_k \geq 0\}_{k=1}^{K}}}{\text{minimize}} && \sum_{l=0}^{L} \text{Tr}(\mathbf{V}_l) + \sum_{k=1}^{K} p_k \\
& \text{subject to} && (20c), (24), (26). \tag{27}
\end{aligned}
$$

This problem is convex and its globally optimal solution can be obtained via, e.g., the interior point method [27] or some off-the-shelf convex optimization tools, e.g., CVX [30]. After solving (27), we update $\bar{\mathbf{Q}}^{(i)}$, $\boldsymbol{\Psi}^{(i)}$, and $\{\boldsymbol{\Phi}_k^{(i)}\}_{k=1}^{K}$ by exploiting the optimal solutions to $\{\{\mathbf{V}_l\}_{l=0}^{L}, \{p_k\}_{k=1}^{K}\}$ and then proceed to the $(i+1)$-th iteration. Furthermore, according to [31], this iterative procedure converges to a Karush-Kuhn-Tucker (KKT) point of the problem in (20).

Upon convergence, we denote the obtained solution as $\{\{\widehat{\mathbf{V}}_l\}_{l=0}^{L}, \{\hat{p}_k\}_{k=1}^{K}\}$. An additional procedure, such as Gaussian randomization [26], is generally exploited for recovering the beamforming vectors $\{\mathbf{v}_l\}_{l=1}^{L}$, i.e., the solution of (19), since $\{\widehat{\mathbf{V}}_l\}_{l=1}^{L}$ may not satisfy the relaxed rank-one constraints in (21). However, the commonly adopted Gaussian randomization for recovering a rank-one solution generally has high computational complexity and leads to certain performance loss. Fortunately, based on the following theorem, we prove that a rank-one solution of (20) can always be constructed from $\{\widehat{\mathbf{V}}_l\}_{l=1}^{L}$ without performance loss.

Theorem 1: Based on the solution $(\{\widehat{\mathbf{V}}_l\}_{l=0}^{L}, \{\hat{p}_k\}_{k=1}^{K})$ in-hand, a solution of (20) achieving the same power consumption as $(\{\widehat{\mathbf{V}}_l\}_{l=0}^{L}, \{\hat{p}_k\}_{k=1}^{K})$ while satisfying the relaxed rank-one constraints in (21) can be constructed as

$$
\mathbf{V}_l^* = \mathbf{v}_l^* (\mathbf{v}_l^*)^H, \ \forall l \geq 1,
$$
$$
\mathbf{V}_0^* = \sum_{l=1}^{L} \widehat{\mathbf{V}}_l + \widehat{\mathbf{V}}_0 - \sum_{l=1}^{L} \mathbf{v}_l^* (\mathbf{v}_l^*)^H,
$$
$$
p_k^* = \hat{p}_k, \ \forall k. \tag{28}
$$

where $\mathbf{v}_l^* = \left(\mathbf{g}_l^H \widehat{\mathbf{V}}_l \mathbf{g}_l \right)^{-1/2} \widehat{\mathbf{V}}_l \mathbf{g}_l, \ \forall l \geq 1$.

Algorithm 1 Proposed Algorithm to Solve (11)

1: *Initialization:* Initialize $\{\{\mathbf{V}_l^{(0)}\}_{l=0}^{L}, \{p_k^{(0)}\}_{k=1}^{K}\}$, iteration index $i = 0$, and convergence accuracy ϵ.
2: **repeat**
3:    Set $i = i + 1$.
4:    Solve (27) with $\{\{\mathbf{V}_l^{(i-1)}\}_{l=0}^{L}, \{p_k^{(i-1)}\}_{k=1}^{K}\}$ and update $\{\{\mathbf{V}_l^{(i)}\}_{l=0}^{L}, \{p_k^{(i)}\}_{k=1}^{K}\}$.
5: **until** *Convergence*.
6: Calculate the transmit beamforming and the uplink transmit power according to (28).
7: Calculate the receive beamformers according to (17) and (18), respectively.
8: *Output:* $\mathbf{u}$, $\{\mathbf{w}_k\}_{k=1}^{K}$, $\{\mathbf{v}_l\}_{l=1}^{L}$, $\mathbf{V}_0$, and $\{p_k\}_{k=1}^{K}$.

Proof: See Appendix B. ∎

Theorem 1 indicates that we can obtain a new solution of (20), i.e., $\{\{\mathbf{V}_l^*\}_{l=0}^{L}, \{p_k^*\}_{k=1}^{K}\}$, which satisfies the rank-one constraints in (21) and attains the same performance as a KKT solution, i.e., $\{\{\widehat{\mathbf{V}}_l\}_{l=0}^{L}, \{\hat{p}_k\}_{k=1}^{K}\}$. Based on $\{\{\mathbf{V}_l^*\}_{l=0}^{L}, \{p_k^*\}_{k=1}^{K}\}$, we thus can recover the solution of (19), i.e., $\{\{\mathbf{v}_l^*\}_{l=1}^{L}, \mathbf{V}_0^*, \{p_k^*\}_{k=1}^{K}\}$. The corresponding receive beamformers are further calculated based on (17) and (18). We summarize the procedure for solving the power minimization problem in (11) as Algorithm 1. Note that the main computational burden of Algorithm 1 stems from solving (27) in each iteration, whose computational complexity is given by $\mathcal{O}\left(N_t^{6.5} L^{3.5} + N_t^4 L^2 K^{1.5} \right)$ [32].

C. Special Case of Uplink Communication Only

The above considered problem involves FD communication. We herein focus on a special case in the absence of downlink communication, i.e., $L = 0$, and the downlink signal is used for target detection only, which is similar to the scenario integrating sensing with uplink communication [18], [19]. The difference is that a fixed communication signal is considered in [18], [19] while we also optimize the uplink transmission here. In this special case, the downlink transmit signal $\mathbf{x}$ and its covariance matrix $\mathbf{Q}$ reduce to

$$
\mathbf{x} = \mathbf{s}_0, \quad \mathbf{Q} = \mathbf{V}_0. \tag{29}
$$

As a result, problem (11) becomes

$$
\begin{aligned}
& \underset{\substack{\mathbf{u}, \{\mathbf{w}_k\}_{k=1}^{K}, \\ \mathbf{V}_0 \succeq \mathbf{0}, \{p_k \geq 0\}_{k=1}^{K}}}{\text{minimize}} && \text{Tr}(\mathbf{V}_0) + \sum_{k=1}^{K} p_k \\
& \text{subject to} && \gamma^{\text{rad}} \geq \tau^{\text{rad}}, \ \gamma_k^{\text{com,UL}} \geq \tau_k^{\text{com,UL}}, \ \forall k. \tag{30}
\end{aligned}
$$

Compared to (11), this problem removes the optimizations on downlink communication and the proposed SCA-based Algorithm 1 is also applicable. However, to solve this simplified problem, we are able to develop an alternative algorithm which dramatically reduces the computational complexity.

Different from Algorithm 1, we consider solving (30) by optimizing $\{\mathbf{u}, \{\mathbf{w}_k\}_{k=1}^{K}\}$ and $\{\mathbf{V}_0, \{p_k\}_{k=1}^{K}\}$ in an alternating manner. Recalling that given $\{\mathbf{V}_0, \{p_k\}_{k=1}^{K}\}$, the optimal solutions to $\{\mathbf{u}, \{\mathbf{w}_k\}_{k=1}^{K}\}$ are obtained in closed-form expressions as shown in Proposition 1, it remains to

optimize $\{\mathbf{V}_0, \{p_k\}_{k=1}^K\}$ with fixed $\{\mathbf{u}, \{\mathbf{w}_k\}_{k=1}^K\}$. Define the following constant terms $\tilde{a}_k \triangleq \mathbf{w}_k^H \mathbf{h}_k \mathbf{h}_k^H \mathbf{w}_k$, $\tilde{\mathbf{b}}_k \triangleq \mathbf{C}^H \mathbf{w}_k$, $\tilde{c}_{k,k'} \triangleq \mathbf{w}_k^H \mathbf{h}_{k'} \mathbf{h}_{k'}^H \mathbf{w}_k, \forall k' \neq k$, and $\tilde{d}_k \triangleq \sigma_r^2 \mathbf{w}_k^H \mathbf{w}_k$ to simplify the notations of $\gamma_k^{\text{com,UL}}$, $\forall k$, in (9). Also, define $\tilde{\mathbf{e}} \triangleq |\beta_0| \mathbf{A}^H(\theta_0) \mathbf{u}$, $\tilde{\mathbf{f}} \triangleq \mathbf{B}^H \mathbf{u}$, $\tilde{g}_k \triangleq \mathbf{u}^H \mathbf{h}_k \mathbf{h}_k^H \mathbf{u}$, $\forall k$, and $\tilde{h} \triangleq \sigma_r^2 \mathbf{u}^H \mathbf{u}$ to simplify γ^{rad} in (7). Then, the subproblem with respect to $\{\mathbf{V}_0, \{p_k\}_{k=1}^K\}$ is expressed as

$$\begin{aligned}
\underset{\substack{\mathbf{V}_0 \succeq \mathbf{0}, \\ \{p_k \geq 0\}_{k=1}^K}}{\text{minimize}} \quad & \text{Tr}(\mathbf{V}_0) + \sum_{k=1}^K p_k \\
\text{subject to} \quad & \frac{\tilde{\mathbf{e}}^H \mathbf{V}_0 \tilde{\mathbf{e}}}{\tilde{\mathbf{f}}^H \mathbf{V}_0 \tilde{\mathbf{f}} + \sum_k p_k \tilde{g}_k + \tilde{h}} \geq \tau^{\text{rad}}, \\
& \frac{p_k \tilde{a}_k}{\tilde{\mathbf{b}}_k^H \mathbf{V}_0 \tilde{\mathbf{b}}_k + \sum_{k' \neq k} p_{k'} \tilde{c}_{k,k'} + \tilde{d}_k} \geq \tau_k^{\text{com,UL}}, \forall k.
\end{aligned}$$
(31)

By rearranging the constraints, this problem is readily transformed into a standard SDP and solved directly. Nonetheless, we will show that (31) is equivalent to an SOCP, which can be solved with much lower computational complexity compared to that of the SDP formulation.

To begin with, we prove the following result regarding (31).

Theorem 2: The optimal solution to (31), denoted by $\{\mathbf{V}_0^*, \{p_k^*\}_{k=1}^K\}$, must satisfy

$$\text{rank}(\mathbf{V}_0^*) = 1.$$
(32)

Proof: See Appendix C. ∎

With Theorem 2, we further obtain the following proposition.

Proposition 2: Let us introduce $\mathbf{v}_0 \in \mathbb{C}^{N_t \times 1}$ and real-valued t_0 and $\{q_k\}_{k=1}^K$ as optimization variables. The optimal solution of (31) can be achieved by solving the following SOCP

$$\begin{aligned}
\underset{\mathbf{v}_0, t_0, \{q_k\}_{k=1}^K}{\text{minimize}} \quad & t_0 \\
\text{subject to} \quad & \begin{bmatrix} \tilde{\mathbf{e}}^H \mathbf{v}_0 \\ \boldsymbol{\varpi} \end{bmatrix} \succeq_C \mathbf{0}, \quad \begin{bmatrix} \sqrt{\tilde{a}_k} q_k \\ \boldsymbol{\varrho}_k \end{bmatrix} \succeq_C \mathbf{0}, \forall k, \\
& \begin{bmatrix} t_0 \\ \mathbf{v}_0 \\ \mathbf{q} \end{bmatrix} \succeq_C \mathbf{0},
\end{aligned}$$
(33)

where $\boldsymbol{\varpi} \triangleq \sqrt{\tau^{\text{rad}}}[\tilde{\mathbf{f}}^H \mathbf{v}_0, \sqrt{\tilde{g}_1} q_1, \cdots, \sqrt{\tilde{g}_K} q_K, \sqrt{\tilde{h}}]^T$, $\boldsymbol{\varrho}_k \triangleq \sqrt{\tau_k^{\text{com,UL}}}[\tilde{\mathbf{b}}_k^H \mathbf{v}_0, \sqrt{\tilde{c}_{k,1}} q_1, \cdots, \sqrt{\tilde{c}_{k,k-1}} q_{k-1}, \sqrt{\tilde{c}_{k,k+1}} q_{k+1}, \cdots, \sqrt{\tilde{c}_{k,K}} q_K, \sqrt{\tilde{d}_k}]^T$, $\forall k$, and $\mathbf{q} \triangleq [q_1, \cdots, q_K]^T$. Denoting the optimal solution of (33) as $\{\mathbf{v}_0^*, t_0^*, \{q_k^*\}_{k=1}^K\}$, we can derive the optimal solution of (31) by $\mathbf{V}_0^* = \mathbf{v}_0^*(\mathbf{v}_0^*)^H$ and $p_k^* = (q_k^*)^2$, $\forall k$.

Proof: See Appendix D. ∎

Proposition 2 provides a computationally efficient approach to find the optimal solution of subproblem (31).

Finally, the proposed low-complexity method for solving (30) is summarized in Algorithm 2. It is easily verified that the objective value of the power consumption is nonincreasing over the iterations and the solution set is compact, thus the proposed algorithm is guaranteed to converge. In terms of computational complexity, in each round of the iteration, the dominating computations of updating $\mathbf{u}^{(i)}$ and $\{\mathbf{w}_k^{(i)}\}_{k=1}^K$ lie in the calculation of matrix inversion, leading to the

---

Algorithm 2 Low-Complexity Solution for (30)

1: *Initialization:* Initialize $\{\mathbf{V}_0^{(0)}, \{p_k^{(0)}\}_{k=1}^K\}$. Set iteration index $i = 0$ and convergence accuracy ϵ.
2: **repeat**
3:     Set $i = i + 1$.
4:     Update $\{\mathbf{u}^{(i)}, \{\mathbf{w}_k^{(i)}\}_{k=1}^K\}$ with $\{\mathbf{V}_0^{(i-1)}, \{p_k^{(i-1)}\}_{k=1}^K\}$ according to (15) and (16), respectively.
5:     Solve the SOCP in (33) with $\{\mathbf{u}^{(i)}, \{\mathbf{w}_k^{(i)}\}_{k=1}^K\}$ and update $\{\mathbf{V}_0^{(i)}, \{p_k^{(i)}\}_{k=1}^K\}$.
6: **until** *Convergence.*
7: *Output:* $\mathbf{u}$, $\{\mathbf{w}_k\}_{k=1}^K$, $\mathbf{V}_0$, and $\{p_k\}_{k=1}^K$.

---

complexity of $\mathcal{O}(KN_t^3)$. For updating $\mathbf{V}_0^{(i)}$ and $\{p_k^{(i)}\}_{k=1}^K$, the complexity of solving the SOCP in (33) is given by $\mathcal{O}(N_t^3 + K^{1.5} N_t)$ [32]. For comparison, we restate the computational complexity of Algorithm 1 in this special case as $\mathcal{O}(N_t^{6.5} + N_t^4 K^{1.5})$. It is found that Algorithm 2 enjoys a much lower order of computational cost than that of Algorithm 1 in each iteration. Furthermore, as will be shown in Section V, these two algorithms share similar convergence speed and performance. Hence, for this special case, Algorithm 2 is an effective alternative to Algorithm 1 with much lower overall complexity.

IV. JOINT FD ISAC DESIGN FOR SUM RATE MAXIMIZATION

In this section, we consider solving (12). Compared to the power minimization criterion, (12) focuses on the sum rate maximization which is generally NP-hard, even in communication-only systems [33]. To solve this difficult problem, we first predetermine the optimal receivers and then develop an effective iterative algorithm.

A. Problem Reformulation

Similarly to the previous section, by predetermining the optimal receive beamformers in (15) and (16) and invoking the equivalent SINR expressions in (17) and (18), we rewrite (12) into the following form:

$$\begin{aligned}
\underset{\substack{\{\mathbf{v}_l\}_{l=1}^L, \mathbf{V}_0 \succeq \mathbf{0}, \\ \{p_k \geq 0\}_{k=1}^K}}{\text{maximize}} \quad & \sum_{k=1}^K \log_2(1 + \bar{\gamma}_k^{\text{com,UL}}) + \sum_{l=1}^L \log_2(1 + \gamma_l^{\text{com,DL}}) \\
\text{subject to} \quad & \bar{\gamma}^{\text{rad}} \geq \tau^{\text{rad}}, \\
& \sum_{l=1}^L \|\mathbf{v}_l\|^2 + \text{Tr}(\mathbf{V}_0) \leq P_{\max}, \\
& p_k \leq P_k, \forall k.
\end{aligned}$$
(34)

By introducing a group of real-valued auxiliary optimization variables $u_k \geq 0$, $\forall k$, and defining $\mathbf{V}_l \triangleq \mathbf{v}_l \mathbf{v}_l^H$, $\forall l$, we further

reformulate (34) as

$$\underset{\substack{\{\mathbf{V}_l \succeq \mathbf{0}\}_{l=0}^{L}, \\ \{p_k \geq 0, u_k \geq 0\}_{k=1}^{K}}}{\text{maximize}} \quad \sum_{k=1}^{K} \log_2(1 + u_k) + \sum_{l=1}^{L} \log_2(1 + \bar{\gamma}_l^{\text{com,DL}})$$

$$\text{subject to} \quad \bar{\gamma}^{\text{rad}} \geq \tau^{\text{rad}}, \ \text{Tr}\left(\sum_{l=0}^{L} \mathbf{V}_l\right) \leq P_{\max},$$

$$u_k \leq \bar{\gamma}_k^{\text{com,UL}}, \ p_k \leq P_k, \ \forall k, \quad (35)$$

where $\bar{\gamma}_l^{\text{com,DL}} = \frac{\mathbf{g}_l^H \mathbf{V}_l \mathbf{g}_l}{\sum_{l'=1, l' \neq l}^{L} \mathbf{g}_l^H \mathbf{V}_{l'} \mathbf{g}_l + \mathbf{g}_l^H \mathbf{V}_0 \mathbf{g}_l + \sigma_l^2}$ and the rank-one constraints of $\{\mathbf{V}_l\}_{l=1}^{L}$ are omitted here. It is easily verified through contradiction that the constraints $u_k \leq \bar{\gamma}_k^{\text{com,UL}}, \ \forall k$, in (35) must keep active at the optimality, which justifies the introduction of $\{u_k\}_{k=1}^{K}$.

B. Proposed Solution

For solving (35), the difficulties lie in the nonconcave term $\sum_{l=1}^{L} \log_2(1 + \bar{\gamma}_l^{\text{com,DL}})$ in the objective function and the nonconvex constraints $\bar{\gamma}^{\text{rad}} \geq \tau^{\text{rad}}$ and $u_k \leq \bar{\gamma}_k^{\text{com,UL}}, \ \forall k$. To tackle the nonconvexity of the objective function, we first rewrite the achievable rate of downlink user l as

$$\log_2(1 + \bar{\gamma}_l^{\text{com,DL}}) = \log_2\left(\sum_{l'=0}^{L} \mathbf{g}_l^H \mathbf{V}_{l'} \mathbf{g}_l + \sigma_l^2\right)$$
$$- \log_2\left(\sum_{l'=0, l' \neq l}^{L} \mathbf{g}_l^H \mathbf{V}_{l'} \mathbf{g}_l + \sigma_l^2\right). \quad (36)$$

Both logarithm functions are concave with respect to $\{\mathbf{V}_l\}_{l=0}^{L}$ and we thus can approximate (36) via linearizing the second term via the iterative SCA approach. Specifically, by exploiting the first-order Taylor expansion, it holds that

$$\log_2\left(\sum_{l'=0, l' \neq l}^{L} \mathbf{g}_l^H \mathbf{V}_{l'} \mathbf{g}_l + \sigma_l^2\right)$$
$$\leq a_l^{(j-1)} + \frac{\log_2 e}{2^{a_l^{(j-1)}}} \sum_{l'=0, l' \neq l}^{L} \mathbf{g}_l^H \left(\mathbf{V}_{l'} - \mathbf{V}_{l'}^{(j-1)}\right) \mathbf{g}_l$$
$$\triangleq \underline{r}_l, \quad (37)$$

where $\mathbf{V}_{l'}^{(j-1)}$ is the solution to $\mathbf{V}_{l'}$ obtained in the $(j-1)$-th iteration, and $a_l^{(j-1)} = \log_2\left(\sum_{l'=0, l' \neq l}^{L} \mathbf{g}_l^H \mathbf{V}_{l'}^{(j-1)} \mathbf{g}_l + \sigma_l^2\right)$. Applying (37), we establish a lower bound of $\log_2(1 + \bar{\gamma}_l^{\text{com,DL}})$ as

$$\log_2(1 + \bar{\gamma}_l^{\text{com}}) \geq \log_2\left(\sum_{l'=0}^{L} \mathbf{g}_l^H \mathbf{V}_{l'} \mathbf{g}_l + \sigma_l^2\right) - \underline{r}_l, \quad (38)$$

which is concave with respect to $\{\mathbf{V}_l\}_{l=0}^{L}$.

Next, we handle the nonconvex constraints. Note that the approximations utilized in Algorithm 1 can still be applied here to deal with these constraints. Specifically, the radar SINR constraint can be tackled as (24). Applying (25) to $u_k \leq \bar{\gamma}_k^{\text{com}}, \ \forall k$, yields

$$\frac{u_k}{p_k} \leq f\left(\mathbf{\Phi}_k, \mathbf{\Phi}_k^{(j-1)}\right), \ \forall k. \quad (39)$$

However, different from (26), the fractional function $\frac{u_k}{p_k}$ in the left-hand side makes constraint (39) still nonconvex. In order to handle this issue, by introducing real-valued auxiliary variables $\{x_k\}_{k=1}^{K}$, we first equivalently transform the single constraint in (39) into two separate constraints as follows:

$$\begin{cases} \frac{x_k^2}{p_k} \leq f\left(\mathbf{\Phi}_k, \mathbf{\Phi}_k^{(j-1)}\right), \\ u_k \leq x_k^2, \end{cases} \quad \forall k. \quad (40)$$

This equivalence is established based on the fact that the constraint $u_k \leq x_k^2$ must keep active at the optimality, which can be verified through contradiction. Then, by replacing the convex function x_k^2 by its first Taylor expansion, we obtain a convex approximation of (40) as

$$\begin{cases} \frac{x_k^2}{p_k} \leq f\left(\mathbf{\Phi}_k, \mathbf{\Phi}_k^{(j-1)}\right), \\ u_k \leq \left(x_k^{(j-1)}\right)^2 + 2x_k^{(j-1)}\left(x_k - x_k^{(j-1)}\right), \end{cases} \quad \forall k, \quad (41)$$

where the variables $\{x_k^{(j-1)}\}_{k=1}^{K}$ are iteratively updated in each iteration.

Now, (35) can be addressed by employing the SCA framework. In particular, in the j-th iteration of the SCA algorithm, we consider the following convex optimization problem

$$\underset{\substack{\{\mathbf{V}_l \succeq \mathbf{0}\}_{l=0}^{L}, \\ \{p_k \geq 0, u_k \geq 0, x_k \geq 0\}_{k=1}^{K}}}{\text{maximize}} \quad \sum_{k=1}^{K} \log_2(1 + u_k)$$
$$+ \sum_{l=1}^{L} \left(\log_2\left(\sum_{l'=0}^{L} \mathbf{g}_l^H \mathbf{V}_{l'} \mathbf{g}_l + \sigma_l^2\right) - \underline{r}_l\right)$$

$$\text{subject to} \quad \text{Tr}\left(\sum_{l=0}^{L} \mathbf{V}_l\right) \leq P_{\max}, \ p_k \leq P_k, \ \forall k,$$
$$(24), (41), \quad (42)$$

whose globally optimal solution can thus be readily found. After solving (42), we update $\bar{\mathbf{Q}}^{(j)}$, $\mathbf{\Psi}^{(j)}$, and $\{\mathbf{\Phi}_k^{(j)}, x_k^{(j)}\}_{k=1}^{K}$. By iteratively solving (42) until convergence, a KKT point of (35) is obtained [31].

Moreover, based on this KKT solution, we can similarly construct a rank-one $\{\mathbf{V}_l^*\}_{l=1}^{L}$ without any performance loss according to Theorem 1. The proof procedure is similar to Appendix B and omitted. Then, the receive beamformers can be calculated according to Proposition 1. The proposed algorithm for solving (12) follows a similar procedure as Algorithm 1 except that in step 4) problem (27) is replaced by problem (42) and we need update $\{\mathbf{V}_l^{(j)}\}_{l=0}^{L}$ and $\{p_k^{(j)}, x_k^{(j)}\}_{k=1}^{K}$. We denote it as Algorithm 3 and no longer present the details for brevity. Moreover, the main computational cost of Algorithm 3 lies in solving (42) in each iteration, whose complexity is $\mathcal{O}\left(N_t^{6.5} L^{3.5} + N_t^4 L^2 K^{1.5}\right)$ [32].

V. SIMULATION RESULTS

A. Parameter Setup

Assume that both the transmit and receive ULAs of the BS have $N_t = N_r = 8$ antennas and are with half-wavelength antenna spacing, i.e., $\frac{d}{\lambda} = \frac{1}{2}$. The BS serves $K = 3$ uplink users and $L = 3$ downlink users. For radar sensing, it is

assumed that the target of interest is located at $\theta_0 = 0°$ and $I = 2$ interferers are located at $\theta_1 = -60°$ and $\theta_2 = 45°$, respectively. The noise powers at the BS and each downlink user are set to $\sigma_r^2 = \sigma_l^2 = -100$ dBm, $\forall l$. We set the maximal transmit power budgets at the BS and each uplink user to $P_{\max} = 15$ dBm and $P_k = 5$ dBm, $\forall k$, respectively. The path loss over distance d m of the user channels is characterized as $\xi = \xi_0(d/d_0)^\kappa$, where ξ_0 stands for the path loss at the reference distance d_0 and κ denotes the path loss exponent. The values of ξ_0, d_0, and κ are set to -30 dB, 1 m, and 3, respectively. For simplicity, we set the distances between the BS and all the users to $d = 200$ m. The small-scale fading of all the user channels are assumed to follow the Rayleigh fading model. Moreover, the channel power gains of the target and the two interferers are set to $|\beta_0|^2 = -100$ dBm and $|\beta_1|^2 = |\beta_2|^2 = -90$ dBm, respectively, such that $\frac{|\beta_0|^2}{\sigma_r^2} = 0$ dB and $\frac{|\beta_1|^2}{\sigma_r^2} = \frac{|\beta_2|^2}{\sigma_r^2} = 10$ dB [17], [24]. For the residual SI channel at the BS, we set $\alpha_{\mathrm{SI}} = -110$ dB and model each entry of $\tilde{\mathbf{H}}_{\mathrm{SI}}$ as a unit-modulus variable with random phase for simplicity [18]. The required SINR thresholds of downlink communications, uplink communications, and target detection are set to $\tau_l^{\mathrm{com,DL}} = 8$ dB, $\forall l$, $\tau_k^{\mathrm{com,UL}} = 5$ dB, $\forall k$, and $\tau^{\mathrm{rad}} = 6$ dB, respectively. All the numerical results are averaged over 200 independent channel realizations.

B. Benchmark Schemes

For performance comparisons, we introduce the following two benchmark schemes.

1) Communication-Only Transmission Scheme: The first scheme considers a communication-only system (noted as "Communication-Only" in the figures) by omitting the sensing SINR constraint when solving problems (11) and (12). This scheme can help evaluate how the integrated sensing functionality affects the communication performance.

2) HD Communication-Based ISAC: To show more explicitly the advantages of FD, we additionally consider a benchmark time-division duplex (TDD) transmission scheme (noted as "HD Mode" in the figures), where the downlink communication and the uplink communication separately occupy two slots while the downlink sensing is continuously performed at the BS for achieving high-accuracy radar sensing (see Appendix E for details).

C. Simulation Results

In this subsection, the performance of the proposed algorithms is evaluated. As exemplified in [34], the authors provided an analytical expression of the target detection probability for the generalized likelihood ratio test detector in a radar system. Invoking the results in [34, Eq. (4) & Eq. (6)], we present the receiver operating characteristic (ROC) curves with different radar SINRs in Fig. 3. It is shown that the detection performance depends on the radar SINR and higher detection probability can be achieved with the growth of SINR. Thereby, the sensing performance in terms of the detection probability of the considered system can be guaranteed by setting a relatively large sensing SINR requirement.
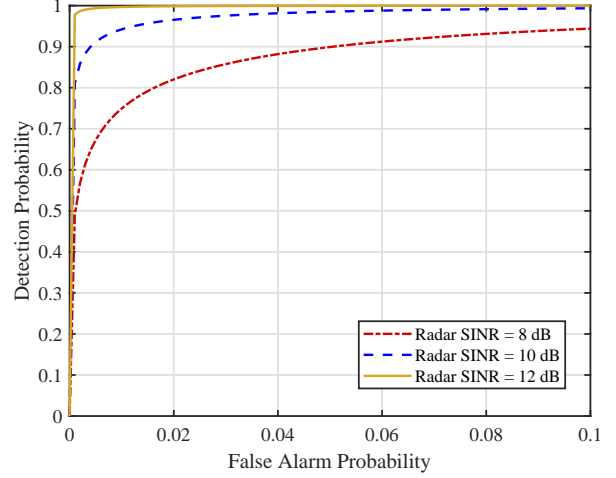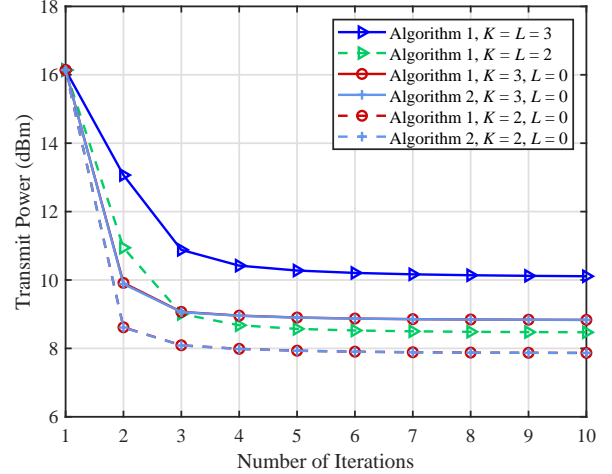

Fig. 3. ROC curves with radar SINRs.

Fig. 4. Convergence performances of Algorithm 1 and Algorithm 2.

Fig. 4 illustrates the convergence performances of Algorithm 1 and Algorithm 2. First, it can be found that with different numbers of users, both algorithms typically converge within 10 iterations. Moreover, it is seen that the power consumption increases with the growth of the number of users, since more transmit power is needed to guarantee the more stringent communication requirements. On the other hand, concerning the curves with $L = 0$ that correspond to the special case discussed in Section III-C, it is seen that Algorithm 1 and Algorithm 2 share the same convergence speed and objective value. Recalling that Algorithm 2 admits a much lower computational complexity per iteration than that of Algorithm 1, the complexity advantage of Algorithm 2 is verified.

In Fig. 5, we show the beampattern gain achieved by Algorithm 1 for solving (11). The beampattern gain, according to [17], is defined by $\frac{|(\mathbf{u}^*)^H \mathbf{A}(\theta) \mathbf{x}^*|^2}{\sigma_r^2 (\mathbf{u}^*)^H \mathbf{u}^*}$, where $\mathbf{u}^*$ and $\mathbf{x}^*$ represent the optimized radar receive beamformer and the transmit
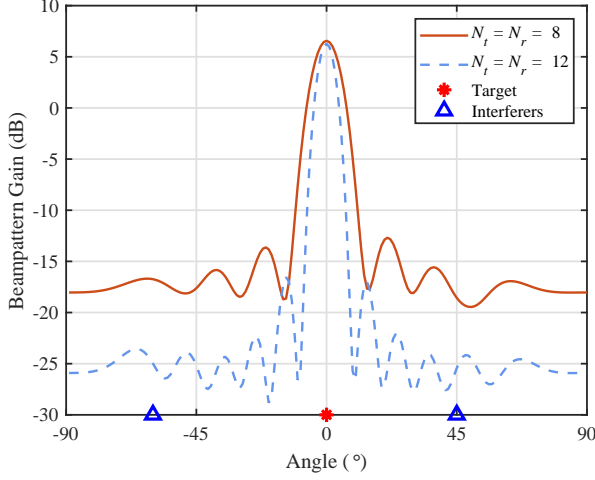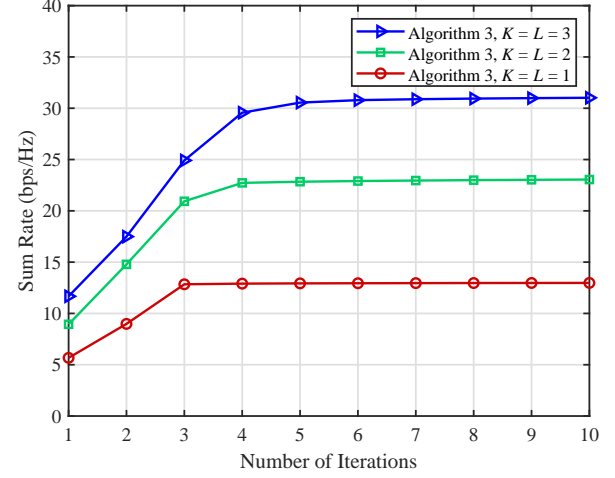
Fig. 5. Beampattern gain achieved by Algorithm 1.
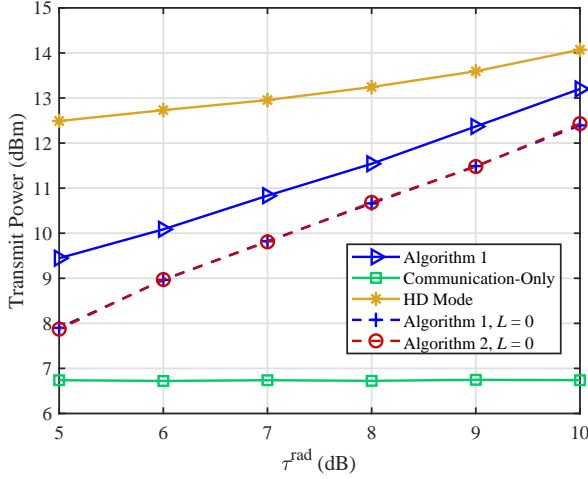

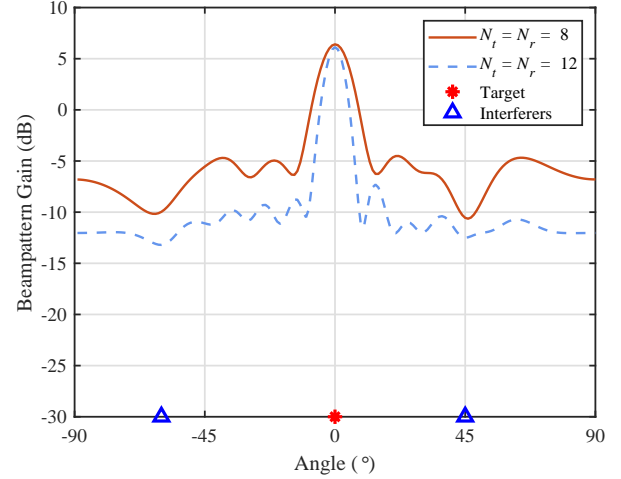Fig. 7. Convergence performance of Algorithm 3.

Fig. 6. Power consumption versus the radar SINR threshold τ^{rad}.

Fig. 8. Beampattern gain achieved by Algorithm 3.

signal, respectively. Obviously, it is seen that the main beam is allocated to the target at direction $\theta_0 = 0°$ and two relatively deep nulls are placed towards the interferers. This indicates the effectiveness of the proposed algorithm. Moreover, when the number of the transceiver antennas increases from 8 to 12, lower power consumption and more precise beampattern can be constructed due to additional DoFs brought by the larger antenna arrays.

Fig. 6 shows the minimum total power versus the radar SINR threshold τ^{rad}. Observe that the power consumed by the communication-only design remains unchanged since it does not contain the sensing constraint. On the contrary, when τ^{rad} increases, the power consumption of Algorithm 1, Algorithm 2, and the HD mode and their performance gaps between the communication-only design are enlarged due to the hasher requirement for radar sensing. Moreover, compared to the conventional HD mode, Algorithm 1 yields a much lower power consumption, which validates the superiority of the proposed FD scheme. Also, it is seen that Algorithm 1

and Algorithm 2 achieve the identical performance in the considered range of parameters.

In the following part, we evaluate the performance of Algorithm 3. First, the convergence performance is illustrated in Fig. 7. It can be seen that the proposed algorithm converges within a few iterations and a higher sum rate is generally obtained with the increasing number of users as the proposed scheme can exploit the inherent multiuser diversity.

Fig. 8 shows the beampattern attained by Algorithm 3. From this figure, it is found that the main beam with a 6 dB gain is towards the target, which is consistent with the result of Fig. 5. However, by comparing Fig. 8 and Fig. 5, we can see that the average value of the beampattern gain achieved by Algorithm 3 is larger than that of Algorithm 1, since the objective of Algorithm 3 is to maximize the sum rate and all the transmit power should be utilized while Algorithm 1 aims to improve the power efficiency and full-power transmission is not always the best strategy.

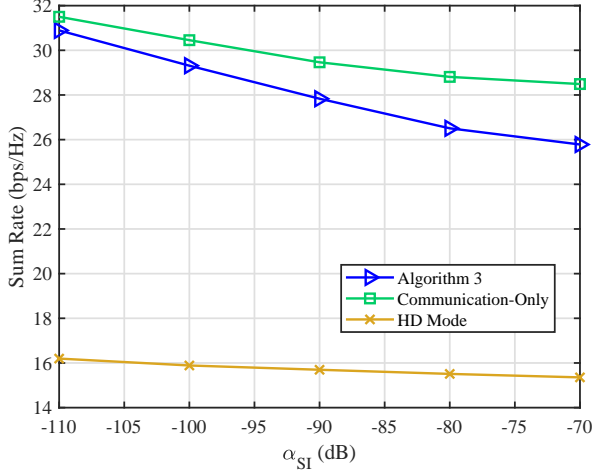Fig. 9 demonstrates the maximum multiuser sum rate versus

Fig. 9. Multiuser sum rate versus the residual SI gain α_{SI}.

the residual SI gain α_{SI}. It can be observed from the figure that when α_{SI} becomes larger, the performance of all three schemes degrades due to the increasing power of the signal-dependent interferences, which conforms to the results in FD communication-only systems [22]. On the other hand, compared to the two FD communication schemes, the achievable rate of the HD mode is less sensitive to the value of α_{SI}, since the uplink and the downlink communications occupy different time slots and only the sensing functionality is affected by the increasing SI power. On the other hand, comparing the two FD communication schemes, we observe that the performance of Algorithm 3 is more sensitive than that of the communication-only scheme. This is because both the FD sensing and communication functionalities in Algorithm 3 are affected by the residual SI gain. When the SI power increases, more downlink transmit powers are consumed for counteracting the effect of SI such that the minimum sensing SINR constraint can be fulfilled, which, however, leads to the communication performance loss. Finally, our proposed advanced scheme with integrating sensing and FD communication can significantly outperform the benchmark HD ISAC scheme. In particular, a nearly double sum rate is attained when the SI power is relatively low.

VI. CONCLUSION

In this paper, we investigated the joint optimization of an FD communication-based ISAC system under the criteria of transmit power minimization and sum rate maximization. For each design problem, we first derived the optimal receive beamformers in closed-form expressions. Then, we developed an effective algorithm to optimize the BS transmit beamforming and the user transmit power based on the SCA technique. Moreover, we also considered a special case for the power minimization criterion and provided a low-cost solution, which enjoys much lower computational complexity compared to the SCA method while achieving almost identical performance. Simulation results verified the effectiveness of the proposed algorithms and showed the tremendous advantages of our

considered FD communication-based ISAC system over the previous frameworks that integrated sensing with HD communication. The performance gains are most notable when the residual SI power is low and the sensing requirement is less restrictive.

APPENDIX A
PROOF OF PROPOSITION 1

We first determine $\mathbf{w}_k$ for maximizing $\gamma_k^{\text{com,UL}}$. Based on the expression in (9), it is found that the maximization of $\gamma_k^{\text{com,UL}}$ belongs to the problem of generalized Rayleigh quotient. Thereby, by invoking the results in [35], we readily obtain the optimal solution to $\mathbf{w}_k$ in (16). To proceed, we optimize $\mathbf{u}$ by rewriting the numerator of γ^{rad} in (7) as

$$
\begin{aligned}
&|\beta_0|^2 \mathbf{u}^H \mathbf{A}(\theta_0)\mathbf{Q}\mathbf{A}(\theta_0)^H \mathbf{u} \\
&= |\beta_0|^2 \mathbf{u}^H \mathbf{a}_r(\theta_0)\mathbf{a}_t^H(\theta_0)\mathbf{Q}\mathbf{a}_t(\theta_0)\mathbf{a}_r^H(\theta_0)\mathbf{u} \\
&= |\beta_0|^2 \mathbf{a}_t^H(\theta_0)\mathbf{Q}\mathbf{a}_t(\theta_0)\mathbf{u}^H\mathbf{a}_r(\theta_0)\mathbf{a}_r^H(\theta_0)\mathbf{u}. \quad (43)
\end{aligned}
$$

Based on the facts that $|\beta_0|^2 \mathbf{a}_t^H(\theta_0)\mathbf{Q}\mathbf{a}_t(\theta_0) \geq 0$ and it is not related to $\mathbf{u}$, we utilize the generalized Rayleigh quotient again to maximize $\frac{\mathbf{u}^H \mathbf{a}_r(\theta_0)\mathbf{a}_r^H(\theta_0)\mathbf{u}}{\mathbf{u}^H\left(\sum_{k=1}^{K} p_k \mathbf{h}_k \mathbf{h}_k^H + \mathbf{B}\mathbf{Q}\mathbf{B}^H + \sigma_r^2 \mathbf{I}_{N_r}\right)\mathbf{u}}$ and arrive at the optimal $\mathbf{u}^*$ in (15).

APPENDIX B
PROOF OF THEOREM 1

The proof follows a similar procedure in the previous work [10]. We divide the proof into two parts. The first part is to show that $\{\{\mathbf{V}_l^*\}_{0=1}^{L}, \{p_k^*\}_{k=1}^{K}\}$ is a feasible solution to (20) and the second part verifies that it achieves the identical performance as $\{\{\widehat{\mathbf{V}}_l\}_{0=1}^{L}, \{\hat{p}_k\}_{k=1}^{K}\}$.

We first prove the feasibility of $\{\{\mathbf{V}_l^*\}_{0=1}^{L}, \{p_k^*\}_{k=1}^{K}\}$. To begin with, it is straightforwardly seen that $\mathbf{V}_l^*$ is positive semidefinite for $l = 1, \cdots, L$. Moreover, given an arbitrary vector $\mathbf{f} \in \mathbb{C}^{N_t \times 1}$, it holds that

$$
\begin{aligned}
\mathbf{f}^H\left(\widehat{\mathbf{V}}_l - \mathbf{v}_l^*\mathbf{v}_l^{*H}\right)\mathbf{f} &= \mathbf{f}^H\left(\widehat{\mathbf{V}}_l - (\mathbf{g}_l^H\widehat{\mathbf{V}}_l\mathbf{g}_l)^{-1}\widehat{\mathbf{V}}_l\mathbf{g}_l\mathbf{g}_l^H\widehat{\mathbf{V}}_l^H\right)\mathbf{f} \\
&= \mathbf{f}^H\widehat{\mathbf{V}}_l\mathbf{f} - (\mathbf{g}_l^H\widehat{\mathbf{V}}_l\mathbf{g}_l)^{-1}|\mathbf{f}^H\widehat{\mathbf{V}}_l\mathbf{g}_l|^2 \\
&\geq \mathbf{f}^H\widehat{\mathbf{V}}_l\mathbf{f} - (\mathbf{g}_l^H\widehat{\mathbf{V}}_l\mathbf{g}_l)^{-1}\mathbf{f}^H\widehat{\mathbf{V}}_l\mathbf{f}\mathbf{g}_l^H\widehat{\mathbf{V}}_l\mathbf{g}_l \\
&= 0, \ \forall l \geq 1, \quad (44)
\end{aligned}
$$

where the inequality follows from the Cauchy-Schwarz inequality. Using (44), together with the fact $\widehat{\mathbf{V}}_0 \succeq \mathbf{0}$, it can be obtained from (28) that $\mathbf{V}_0^* \succeq \mathbf{0}$. Thus, we have $\{\mathbf{V}_l^* \succeq \mathbf{0}\}_{0=1}^{L}$. To proceed, it follows from (28) that

$$
\sum_{l=1}^{L}\widehat{\mathbf{V}}_l + \widehat{\mathbf{V}}_0 = \sum_{l=1}^{L}\mathbf{V}_l^* + \mathbf{V}_0^*. \quad (45)
$$

This equality, together with the unchanged values of $\{p_k\}_{k=1}^{K}$, implies that $\{\{\widehat{\mathbf{V}}_l\}_{0=1}^{L}, \{\hat{p}_k\}_{k=1}^{K}\}$ and $\{\{\mathbf{V}_l^*\}_{0=1}^{L}, \{p_k^*\}_{k=1}^{K}\}$ yield the same $\bar{\mathbf{Q}}$, $\mathbf{\Psi}$, and $\{\mathbf{\Phi}_k\}_{k=1}^{K}$. Moreover, it is verified that

$$
\begin{aligned}
\mathbf{g}_l^H\mathbf{V}_l^*\mathbf{g}_l &= \mathbf{g}_l^H\mathbf{v}_l^*\mathbf{v}_l^{*H}\mathbf{g}_l \\
&= (\mathbf{g}_l^H\widehat{\mathbf{V}}_l\mathbf{g}_l)^{-1}\mathbf{g}_l^H\widehat{\mathbf{V}}_l\mathbf{g}_l\mathbf{g}_l^H\widehat{\mathbf{V}}_l^H\mathbf{g}_l \\
&= \mathbf{g}_l^H\widehat{\mathbf{V}}_l\mathbf{g}_l, \ \forall l. \quad (46)
\end{aligned}
$$

Therefore, constraints (20a), (20b), and (20c) also hold for $\{\{\mathbf{V}_l^*\}_{0=1}^L, \{p_k^*\}_{k=1}^K\}$. The first part is proven.

We then prove that the objective values of $\{\{\mathbf{V}_l^*\}_{0=1}^L, \{p_k^*\}_{k=1}^K\}$ and $\{\{\widehat{\mathbf{V}}_l\}_{0=1}^L, \{\hat{p}_k\}_{k=1}^K\}$ are identical. Applying (28), we immediately have $\sum_{l=0}^L \text{Tr}(\widehat{\mathbf{V}}_l) + \sum_{k=1}^K \hat{p}_k = \sum_{l=0}^L \text{Tr}(\mathbf{V}_l^*) + \sum_{k=1}^K p_k^*$. The second part of proof is completed.

APPENDIX C
PROOF OF THEOREM 2

We accomplish the proof by analyzing the KKT conditions of the problem in (31). Since (31) is a convex SDP and the Slater's condition holds, the duality gap is zero and the KKT conditions are sufficient and necessary for guaranteeing the optimality [27]. Let $\mu \geq 0$, $\{\lambda_k \geq 0\}_{k=1}^K$, and a positive semidefinite matrix $\mathbf{Z} \succeq \mathbf{0}$ denote the Lagrange multipliers associated with the radar SINR constraint, the uplink communication SINR constraints, and the semidefinition constraint $\mathbf{V}_0 \succeq \mathbf{0}$, respectively. Thus, the partial Lagrangian function of (31) is given by

$$
\begin{aligned}
&\mathcal{L}(\mathbf{V}_0, \{p_k\}_{k=1}^K, \mu, \{\lambda_k\}_{k=1}^K, \mathbf{Z}) \\
&= \text{Tr}(\mathbf{V}_0) + \sum_{k=1}^K p_k + \mu(\tilde{\mathbf{f}}^H \mathbf{V}_0 \tilde{\mathbf{f}} + \sum_k \tilde{g}_k p_k + \tilde{h} - \frac{1}{\tau^{\text{rad}}} \tilde{\mathbf{e}}^H \mathbf{V}_0 \tilde{\mathbf{e}}) \\
&+ \sum_{k=1}^K \lambda_k (\tilde{\mathbf{b}}_k^H \mathbf{V}_0 \tilde{\mathbf{b}}_k + \sum_{k' \neq k} \tilde{c}_{k,k'} p_{k'} + \tilde{d}_k - \frac{1}{\tau^{\text{com,UL}}} \tilde{a}_k p_k) \\
&- \text{Tr}(\mathbf{Z} \mathbf{V}_0).
\end{aligned} \tag{47}
$$

Given the Lagrangian function, we further obtain the dual function of problem (31) by

$$
\begin{aligned}
&g(\mu, \{\lambda_k\}_{k=1}^K, \mathbf{Z}) \\
&= \inf_{\mathbf{V}_0, \{p_k > 0\}_{k=1}^K} \mathcal{L}(\mathbf{V}_0, \{p_k\}_{k=1}^K, \mu, \{\lambda_k\}_{k=1}^K, \mathbf{Z}) \\
&= \inf_{\mathbf{V}_0, \{p_k > 0\}_{k=1}^K} \text{Tr}(\mathbf{B} \mathbf{V}_0) + f(\{p_k\}_{k=1}^K),
\end{aligned} \tag{48}
$$

where $\mathbf{B} = \mathbf{I}_{N_t} + \mu \tilde{\mathbf{f}} \tilde{\mathbf{f}}^H + \sum_{k=1}^K \lambda_k \mathbf{b}_k \mathbf{b}_k^H - \frac{\mu}{\tau^{\text{rad}}} \tilde{\mathbf{e}} \tilde{\mathbf{e}}^H - \mathbf{Z}$ and $f(\{p_k\}_{k=1}^K)$ contains the remaining terms related to $\{p_k\}_{k=1}^K$. In order to guarantee a bounded dual optimal value, it follows from (48) that $\mathbf{B} = \mathbf{0}$, which means that

$$
\mathbf{Z} = \mathbf{I}_{N_t} + \mu \tilde{\mathbf{f}} \tilde{\mathbf{f}}^H + \sum_{k=1}^K \lambda_k \mathbf{b}_k \mathbf{b}_k^H - \frac{\mu}{\tau^{\text{rad}}} \tilde{\mathbf{e}} \tilde{\mathbf{e}}^H. \tag{49}
$$

Furthermore, due to the non-negativeness of μ and $\{\lambda_k\}_{k=1}^K$, we can infer from (49) that $\text{rank}(\mathbf{Z}) \geq N_t - 1$. On the other hand, we list the related KKT conditions of problem (31) for the proof as follows:

$$
\frac{1}{\tau^{\text{rad}}} \tilde{\mathbf{e}}^H \mathbf{V}_0^* \tilde{\mathbf{e}} \geq \tilde{\mathbf{f}}^H \mathbf{V}_0^* \tilde{\mathbf{f}} + \sum_k \tilde{g}_k p_k^* + \tilde{h}, \tag{50}
$$

$$
\mathbf{Z}^* \mathbf{V}_0^* = \mathbf{0}. \tag{51}
$$

Combining $\text{rank}(\mathbf{Z}) \geq N_t - 1$ and (51), we have $\text{rank}(\mathbf{V}_0^*) \leq 1$. Moreover, condition (50) holds only when $\text{rank}(\mathbf{V}_0^*) \neq 0$ since $\tilde{h} > 0$. Thereby, we conclude that $\text{rank}(\mathbf{V}_0^*) = 1$.

APPENDIX D
PROOF OF PROPOSITION 2

It follows from Theorem 2 that we can express $\mathbf{V}_0$ by $\mathbf{V}_0 = \mathbf{v}_0 \mathbf{v}_0^H$ without loss of optimality, where $\mathbf{v}_0 \in \mathbb{C}^{N_t \times 1}$ represents the radar beamformer. Denoting $q_k = \sqrt{p_k} \geq 0$, $\forall k$, problem (31) is recast as

$$
\begin{aligned}
\underset{\mathbf{v}_0, \{q_k\}_{k=1}^K}{\text{minimize}} \quad & \|\mathbf{v}_0\|^2 + \sum_{k=1}^K q_k^2 \\
\text{subject to} \quad & \frac{|\tilde{\mathbf{e}}^H \mathbf{v}_0|^2}{|\tilde{\mathbf{f}}^H \mathbf{v}_0|^2 + \sum_k \tilde{g}_k q_k^2 + \tilde{h}} \geq \tau^{\text{rad}}, \\
& \frac{\tilde{a}_k q_k^2}{|\tilde{\mathbf{b}}_k^H \mathbf{v}_0|^2 + \sum_{k' \neq k} \tilde{c}_{k,k'} q_{k'}^2 + \tilde{d}_k} \geq \tau_k^{\text{com,UL}}, \ \forall k.
\end{aligned} \tag{52}
$$

For (52), it can be verified that rotating the optimal $\mathbf{v}_0$ with an arbitrary phase scaling does not destroy the optimality. Therefore, focusing on the radar SINR in the first constraint of (52), it is without loss of optimality to further restrict $\mathcal{I}\{\tilde{\mathbf{e}}^H \mathbf{v}_0\} = 0$. Then, we can take the square root of $|\tilde{\mathbf{e}}^H \mathbf{v}_0|^2$ and transform the first constraint in (52) to $\tilde{\mathbf{e}}^H \mathbf{v}_0 \geq \|\boldsymbol{\varpi}\|$, where $\boldsymbol{\varpi} \triangleq \sqrt{\tau^{\text{rad}}} \left[\tilde{\mathbf{f}}^H \mathbf{v}_0, \sqrt{\tilde{g}_1} q_1, \cdots, \sqrt{\tilde{g}_K} q_K, \sqrt{\tilde{h}} \right]^T$. It can be further rewritten as the following SOC $\begin{bmatrix} \tilde{\mathbf{e}}^H \mathbf{v}_0 \\ \boldsymbol{\varpi} \end{bmatrix} \succeq_C \mathbf{0}$, where the notation $\succeq_C$ denotes the generalized inequality as $\begin{bmatrix} z \\ \mathbf{z} \end{bmatrix} \succeq_C \mathbf{0} \iff \|\mathbf{z}\| \leq z$ [36]. To proceed, performing the similar operations for the communication SINR constraints in (52) yields the second set of SOCs in (33). Finally, by introducing an auxiliary variable $t > 0$, the minimization of $\|\mathbf{v}_0\|^2 + \sum_{k=1}^K q_k^2$ is equivalent to minimize t with an additional constraint $t \geq \|\mathbf{v}_0\|^2 + \sum_{k=1}^K q_k^2$. Then, denoting $t_0 = \sqrt{t}$, (52) is transformed into the SOCP given in (33).

APPENDIX E
DETAILS OF THE TDD BENCHMARK SCHEME

Assume that the uplink and downlink time slots have the same duration. In the downlink slot, the BS transmits an ISAC signal $\mathbf{x}$ and receives the radar echo signal adopting a linear beamformer $\mathbf{u}$. The involved optimization problems of transmit power minimization and sum rate maximization take the form:

$$
\begin{aligned}
(\mathcal{P}_{\text{minP}}^{\text{HD,DL}}): \quad \underset{\{\mathbf{v}_l\}_{l=1}^L, \mathbf{V}_0 \succeq \mathbf{0}, \mathbf{u}}{\text{minimize}} \quad & \sum_{l=1}^L \|\mathbf{v}_l\|^2 + \text{Tr}(\mathbf{V}_0) \\
\text{subject to} \quad & \gamma_{\text{HD}}^{\text{rad,DL}} \geq \tau^{\text{rad}}, \\
& \gamma_l^{\text{com,DL}} \geq \bar{\tau}_l^{\text{com,DL}}, \ \forall l.
\end{aligned} \tag{53}
$$

$$
\begin{aligned}
(\mathcal{P}_{\text{maxR}}^{\text{HD,DL}}): \quad \underset{\{\mathbf{v}_l\}_{l=1}^L, \mathbf{V}_0 \succeq \mathbf{0}, \mathbf{u}}{\text{maximize}} \quad & \sum_{l=1}^L \log_2(1 + \gamma_l^{\text{com,DL}}) \\
\text{subject to} \quad & \gamma_{\text{HD}}^{\text{rad,DL}} \geq \tau^{\text{rad}}, \\
& \sum_{l=1}^L \|\mathbf{v}_l\|^2 + \text{Tr}(\mathbf{V}_0) \leq P_{\text{max}},
\end{aligned} \tag{54}
$$

respectively. Here, $\gamma_{\text{HD}}^{\text{rad,DL}} = \frac{|\beta_0|^2 \mathbf{u}^H \mathbf{A}(\theta_0)\mathbf{QA}(\theta_0)^H \mathbf{u}}{\mathbf{u}^H (\mathbf{BQB}^H + \sigma_r^2 \mathbf{I}_{N_r})\mathbf{u}}$ represents the radar SINR without the interference from the uplink transmission due to the HD mode and $\bar{\tau}_l^{\text{com,DL}} \triangleq (1+\tau_l^{\text{com,DL}})^2 - 1$ ensures that the minimum data rate of downlink user l achieved in the HD scheme equals to that of the FD case. In the uplink slot, the BS simultaneously receives the communication signal from K uplink users and transmits $\mathbf{s}_0$ for downlink sensing. The joint optimization problems are written as

$$(\mathcal{P}_{\text{minP}}^{\text{HD,UL}}): \underset{\mathbf{V}_0 \succeq \mathbf{0}, \{\mathbf{w}_k, p_k\}_{k=1}^K}{\text{minimize}} \text{Tr}(\mathbf{V}_0) + \sum_{k=1}^K p_k$$
$$\text{subject to} \quad \gamma^{\text{rad}} \geq \tau^{\text{rad}},$$
$$\gamma_k^{\text{com,UL}} \geq \bar{\tau}_k^{\text{com,UL}}, \ \forall k. \quad (55)$$

$$(\mathcal{P}_{\text{maxR}}^{\text{HD,UL}}): \underset{\mathbf{V}_0 \succeq \mathbf{0}, \{\mathbf{w}_k, p_k\}_{k=1}^K}{\text{maximize}} \sum_{k=1}^K \log_2(1 + \gamma_k^{\text{com,UL}})$$
$$\text{subject to} \quad \gamma^{\text{rad}} \geq \tau^{\text{rad}},$$
$$\text{Tr}(\mathbf{V}_0) \leq P_{\max},$$
$$p_k \leq P_k, \ \forall k, \quad (56)$$

respectively, where $\bar{\tau}_k^{\text{com,UL}} \triangleq (1+\tau_l^{\text{com,UL}})^2 - 1$ guarantees that the minimum uplink user data rates in both FD and HD cases are identical. All the four problems can be solved using the proposed algorithms with some minor modifications. Denote the optimized objective values of these four problems as P^{DL}, R^{DL}, P^{UL}, and R^{UL}, respectively. We finally obtain the average power consumption and achievable rate of this TDD system by $\frac{1}{2}(P^{\text{DL}} + P^{\text{UL}})$ and $\frac{1}{2}(R^{\text{DL}} + R^{\text{UL}})$, respectively.

REFERENCES

[1] Z. He *et al.*, "Integrated sensing and full-duplex communication: Joint transeiver beamforming and power allocation," submitted to *Proc. IEEE Int. Conf. Acoust., Speech Signal Process. (ICASSP)*, Jun. 2023.

[2] W. Xu *et al.*, "Edge learning for B5G networks with distributed signal processing: Semantic communication, edge computing, and wireless sensing," 2022. Available: https://arxiv.org/pdf/2206.00422.pdf

[3] W. Shi, W. Xu, X. You, C. Zhao, and K. Wei, "Intelligent reflection enabling technologies for integrated and green Internet-of-Everything beyond 5G: Communication, sensing, and security," *IEEE Wireless Commun.*, early access, May 09, 2022, doi: 10.1109/MWC.018.2100717.

[4] J. A. Zhang *et al.*, "An overview of signal processing techniques for joint communication and radar sensing," *IEEE J. Sel. Topics Signal Process.*, vol. 15, no. 6, pp. 1295–1315, Nov. 2021.

[5] J. A. Zhang *et al.*, "Enabling joint communication and radar sensing in mobile networks—A survey," *IEEE Commun. Surveys Tuts.*, vol. 24, no. 1, pp. 306–345, 1st Quart. 2022.

[6] F. Liu *et al.*, "Integrated sensing and communications: Towards dual-functional wireless networks for 6G and beyond," *IEEE J. Sel. Areas Commun.*, vol. 40, no. 6, pp. 1728–1767, Jun. 2022.

[7] J. Li and P. Stoica, "MIMO radar with colocated antennas," *IEEE Signal Process. Mag.*, vol. 24, no. 5, pp. 106–114, Sep. 2007.

[8] P. Stoica, J. Li, and Y. Xie, "On probing signal design for MIMO radar," *IEEE Trans. Signal Process.*, vol. 55, no. 8, pp. 4151–4161, Aug. 2007.

[9] F. Liu *et al.*, "MU-MIMO communications with MIMO radar: From coexistence to joint transmission," *IEEE Trans. Wireless Commun.*, vol. 17, no. 4, pp. 2755–2770, Apr. 2018.

[10] X. Liu, T. Huang, N. Shlezinger, Y. Liu, J. Zhou, and Y. C. Eldar, "Joint transmit beamforming for multiuser MIMO communications and MIMO radar," *IEEE Trans. Signal Process.*, vol. 68, pp. 3929–3944, Jun. 2020.

[11] H. Hua, J. Xu, and T. X. Han, "Optimal transmit beamforming for integrated sensing and communication," 2021. Available: https://arxiv.org/pdf/2104.11871.pdf

[12] Z. Lyu, G. Zhu, and J. Xu, "Joint maneuver and beamforming design for UAV-enabled integrated sensing and communication," *IEEE Trans. Wireless Commun.*, early access, Oct. 11, 2022, doi: 10.1109/TWC.2022.3211533.

[13] Z. He, W. Xu, H. Shen, Y. Huang, and H. Xiao, "Energy efficient beamforming optimization for integrated sensing and communication," *IEEE Wireless Commun. Lett.*, Vol. 11, no. 7, pp. 1374–1378, Jul. 2022.

[14] F. Liu, Y.-F. Liu, A. Li, C. Masouros, and Y. C. Eldar, "Cramér-rao bound optimization for joint radar-communication beamforming," *IEEE Trans. Signal Process.*, vol. 70, pp. 240–253, Jan. 2022.

[15] J. Pritzker, J. Ward, and Y. C. Eldar, "Transmit precoder design approaches for dual-function radar-communication systems," 2022. Available: https://arxiv.org/pdf/2203.09571.pdf

[16] L. Chen, Z. Wang, Y. Du, Y. Chen, and F. Richard Yu, "Generalized transceiver beamforming for DFRC with MIMO radar and MU-MIMO communication," *IEEE J. Sel. Areas Commun.*, Vol. 40, no. 6, pp. 1795–1808, Jun. 2022.

[17] C. G. Tsinos, A. Arora, S. Chatzinotas, and B. Ottersten, "Joint transmit waveform and receive filter design for dual-function radar-communication systems," *IEEE J. Sel. Topics Signal Process.*, vol. 15, no. 6, pp. 1378–1392, Nov. 2021.

[18] M. Temiz, E. Alsusa, and M. W. Baidas, "A dual-function massive MIMO uplink OFDM communication and radar architecture," *IEEE Trans. Cogn. Commun. Netw.*, vol. 8, no. 2, pp. 750–762, Jun. 2022.

[19] X. Wang, Z. Fei, J. A. Zhang, and J. Huang, "Sensing-assisted secure uplink communications with full-duplex base station," *IEEE Commun. Lett.*, vol. 26, no. 2, pp. 249–253, Feb. 2022.

[20] C. B. Barneto, S. D. Liyanaarachchi, M. Heino, T. Riihonen, and M. Valkama, "Full duplex radio/radar technology: The enabler for advanced joint communication and sensing," *IEEE Wireless Commun.*, vol. 28, no. 1, pp. 82–88, Feb. 2021.

[21] C. B. Barneto *et al.*, "Full-duplex OFDM radar with LTE and 5G NR waveforms: Challenges, solutions, and measurements," *IEEE Trans. Microwave Theory and Techniques,* vol. 67, no. 10, pp. 4042–4054, Oct. 2019.

[22] A. Sabharwal, P. Schniter, D. Guo, D. W. Bliss, S. Rangarajan, and R. Wichman, "In-band full-duplex wireless: Challenges and opportunities," *IEEE J. Sel. Areas Commun.*, vol. 32, no. 9, pp. 1637–1652, Sep. 2014.

[23] C.-Y. Chen and P. P. Vaidyanathan, "MIMO radar waveform optimization with prior information of the extended target and clutter," *IEEE Trans. Signal Process.*, vol. 57, no. 9, pp. 3533–3544, Sep. 2009.

[24] L. Wu, P. Babu, and D. P. Palomar, "Transmit waveform/receive filter design for MIMO radar with multiple waveform constraints," *IEEE Trans. Signal Process.*, vol. 66, no. 6, pp. 1526–1540, Mar. 2018.

[25] G. Cui, H. Li, and M. Rangaswamy, "MIMO radar waveform design with constant modulus and similarity constraints," *IEEE Trans. Signal Process.*, vol. 62, no. 2, pp. 343–353, Jan. 2014.

[26] Z.-Q. Luo, W.-K. Ma, A. M.-C. So, Y. Ye, and S. Zhang, "Semidefinite relaxation of quadratic optimization problems," *IEEE Signal Process. Mag.*, vol. 27, no. 3, pp. 20–34, May 2010.

[27] S. Boyd and L. Vandenberghe, *Convex Optimization*. Cambridge, U.K.: Cambridge Univ. Press, 2004.

[28] T. Lipp and S. Boyd, "Variations and extension of the convex-concave procedure," *Optim. Eng.*, vol. 17, no. 2, pp. 263–278, Jun. 2016.

[29] A. Hjoungnes, *Complex-Valued Matrix Derivatives: With Applications in Signal Processing and Communications*. Cambridge, U.K.: Cambridge Univ. Press, 2011.

[30] M. Grant and S. Boyd. (Dec. 2018). *CVX: MATLAB Software for Disciplined Convex Programming.* [Online]. Available: http://cvxr.com/cvx/

[31] A. Beck, A. Ben-Tal, and L. Tetruashvili, "A sequential parametric convex approximation method with applications to nonconvex truss topology design problems," *J. Global Optim.*, vol. 47, no. 1, pp. 29–51, May 2010.

[32] K.-Y. Wang, A. M.-C. So, T.-H. Chang, W.-K. Ma, and C.-Y. Chi, "Outage constrained robust transmit optimization for multiuser MISO downlinks: Tractable approximations by conic optimization," *IEEE Trans. Signal Process.*, vol. 62, no. 21, pp. 5690–5705, Nov. 2014.

[33] Z.-Q. Luo and S. Zhang, "Dynamic spectrum management: Complexity and duality," *IEEE J. Sel. Topics Signal Process.,* vol. 2, no. 1, pp. 57–73, Feb. 2008.

[34] A. De Maio *et al.*, "Code design to optimize radar detection performance under accuracy and similarity constraints," *IEEE Trans. Signal Process.*, vol. 56, no. 11, pp. 5618–5629, Nov. 2008.

[35] G. H. Golub and C. F. Van Loan, *Matrix Computations*, 3rd ed. Baltimore, MD, USA: Johns Hopkins Univ. Press, 1996.

[36] A. Wiesel, Y. C. Eldar, and S. Shamai (Shitz), "Linear precoding via conic optimization for fixed MIMO receivers," *IEEE Trans. Signal Process.*, vol. 54, no. 1, pp. 161–176, Jan. 2006.